11-4-2015

# Evaluating Corrosion Resistance of Reinforcing Steel in a Novel Green Concrete

Andrea Carolina Ramirez
*University of South Florida*, andreacaroli@mail.usf.edu

Evaluating Corrosion Resistance of Reinforcing Steel in a Novel Green Concrete

by

Andrea C Ramirez M.

A thesis submitted in partial fulfillment
of the requirements for the degree of
Master of Science in Engineering Science
Department of Civil and Environmental Engineering
College of Engineering
University of South Florida

Major Professor: Alberto Sagüés, Ph.D.
Sarina Ergas, Ph.D.
Qiong Zhang, Ph.D.

Date of Approval:
October 26, 2015

Keywords: durability, novel cement, carbon dioxide sequestration, greenhouse gas emissions, sustainability

## DEDICATION

This thesis is dedicated to the memory of my beloved grandmother Elena, for being such an admirable person and most importantly for her unconditional love. To my husband, parents and sisters. Family is everything and I am what I am because of them. This Thesis is for them, they are my everyday inspiration and motivation. Thank you for loving me and helping me to become a better person every day.

**ACKNOWLEDGMENTS**

Immeasurable appreciation and deepest gratitude for the help and support are extended to the following persons who directly or indirectly have contributed to making this Thesis possible.

Dr. Sarina Ergas for her valuable support and for seeing my potential as a Graduate Research Assistant for the Corrosion Laboratory.

Distinguished Professor Alberto A. Sagüés, for giving me the opportunity to work in his group of research and being an excellent mentor, for always motivating me to become a better professional, for his continuance guidance and support. Thank you.

Enrique Paz and Mike Walsh, for their helpful assistance and guidance at all stages of the project. Ihab Taha and Chiggy Tafadswa, for helping me with gathering data, your collaboration has been highly appreciated.

Leonidas Emmenegger, Jacob Bumgardner, Joe Fernandez, William Ruth and Brittany Kociuba, for their support every day in the laboratory.

Solidia Technologies, for providing support for this project under a research contract with the University of South Florida.

The opinions, findings and conclusions are those of the author and do not necessarily intend to represent those of the sponsoring organization.

**TABLE OF CONTENTS**

## LIST OF TABLES

**LIST OF FIGURES**

**ABSTRACT**

Reinforced concrete structures are expected to have a long service life with minimal maintenance. Corrosion of reinforcing steel is a major factor in reducing concrete structure lifespan, as corrosion products occupy a larger volume than that of the consumed steel and generate tensile stresses that crack the concrete cover. Procedures to control corrosion in traditional concrete, which is made with Portland-cement (PC), have been well established. However, in recent years novel concrete materials based on alternatives to normally cured PC have been developed in response to global needs to reduce greenhouse gases emissions. In particular, a promising new cement has emerged that cures into concrete in a $CO_2$/water environment resulting in a silica and calcium carbonate matrix. This material has the potential to lower the release of greenhouse gases into the environment at the time that provides a more efficient use of resources. This new material poses a reinforcement corrosion control challenge because unlike PC based materials, the pore water of the carbonated material has a significantly lower pore water pH value, thus making it more difficult to retain a stable passive film. On the other hand, other properties of the new material, including high electric resistivity, may contribute in mitigating the corrosion process. The corrosion behavior of steel reinforcement in these circumstances needs to be investigated.

To evaluate the corrosion behavior of steel in concrete, plain steel rebars were tested with various surface finishes including: as received (mill scale), sandblasted and epoxy coated with intentional coating breaks. The specimens were exposed to environments including fresh distilled water, mildly corrosive water, salt water and an atmospheric environment with 85% relative

humidity. The open circuit potential was monitored to determine the time when the activation of the steel surface likely occurred. The corrosion rate of the specimens was determined by means of electrochemical impedance spectroscopy (EIS), the applicability of this technique to corrosion evaluation in novel cementitious media is discussed as well.

Specimens exposed to air at 85% RH appeared to retain a passive steel condition during the entire exposure period. Apparent corrosion rates (ACR) were extremely low. Pending confirmation by prolonged testing, this result is encouraging for applications such as indoor hollow slabs and similar structural components not subject to direct wetting.

Specimens exposed to immersion regimes in Fresh, Mild and Salt water media showed signs of activation after a very short time (days-week) of exposure. Corrosion assessment thus occurred predominantly in the corrosion propagation stage. Early activation is thought to reflect a combination of rapid water absorption and only moderately alkaline pH (~8.8) of the concrete assessed.

The ACRs for plain and sandblasted rebar in the Fresh and Mild water regimes were very low, e.g, < 2 μm/y. If confirmed by further evaluation, applications for contact with fresh natural water with moderate service life needs might in principle be achievable. The novel concrete assessed here exhibited much higher resistivity values than conventional PC concrete under similar conditions. This higher resistivity may have been an important factor in limiting corrosion rate.

ACRs or plain and sandblasted rebar in the salt water exposure were initially significantly greater that those indicated above, as expected, given the highly aggressive nature of the medium. Those ACR values, if sustained, would cause concrete cracking in an OPC application in a short time, on the order of only a few years. ACRs however decreased with exposure time;

those results need careful follow up evaluation for possible artifacts such as excessive water pickup from salt deliquescence, which could have transport-limited the rate of the cathodic reaction.

ACRs of epoxy-coated rebar specimens were extremely small in all test conditions. However, this result may stem from limitations of the EIS tests to detect undercoating corrosion and interpretation of this finding needs to be postponed until future autopsy of test specimens.

The investigation illustrated an array of methodologies that can be deployed to evaluate the corrosion performance of reinforcement in new media and provide a framework for extended investigations.

# CHAPTER 1: INTRODUCTION

## Cement

Cement is a finely ground powder that sets to a hard mass when mixed with water [1]. It is commonly referred to, as the binding material used in infrastructure and civil engineering construction, with its most common application being the adhesive within concrete. Cement is a material of diverse chemical composition, nonetheless, the most widely used is ordinary Portland cement (OPC). The extensive availability and low cost of cement makes it one of the most widely used materials in the world [2].

PC consists mainly of compounds of lime (calcium oxide, CaO), mixed with silica (silicon dioxide, $SiO_2$) and alumina (aluminum oxide, $Al_2O_3$) [1]. High quality cements require raw materials of high purity and uniform composition. Limestone (calcium carbonate, $CaCO_3$) is the most common source of calcium oxide, although other forms of calcium carbonate can be used. Iron-bearing aluminosilicates are commonly used as the primary source of silica [3].

## Carbon Dioxide Emissions from the Cement Manufacturing Process

The emission of carbon dioxide ($CO_2$) in industrial processes represents an increasing concern due to the various ways $CO_2$ impacts the environment, predominately through climate change. Organizations and companies are taking this concern more seriously, goals and standards are being set to reduce the $CO_2$ emissions in manufacturing processes. In 2013, the global $CO_2$ emissions due to fossil fuel use and cement production were 36 Gtons. Specifically, the emissions from the cement industry accounted for 5.5% of global $CO_2$ emissions [4]. Additionally, with the expected increase in population, concrete demand from the construction

industry is anticipated to rise. Therefore, if no other alternative is considered, the carbon footprint of the PC industry will continue to surge.

Cement production accounts for the majority of the $CO_2$ emissions associated with concrete. Unlike other materials, 40% of the $CO_2$ emitted during cement production is related to fuel and electricity [2, 5]. The remaining 60% is emitted as a byproduct of clinker production. During this process, the calcium carbonate is calcinated and converted to lime, the primary component of cement. The simplified stoichiometric relationship is shown below:

$$CaCO_3 \xrightarrow{\Delta} CaO + CO_2 \quad (1)$$

**Reducing Carbon Dioxide Emissions in the Cement Manufacturing Process**

There is increasing awareness of the need to reduce the emission of $CO_2$ in the cement production process. Considering that 60% of the emissions come from the use of limestone, altering the usage of this material is a promising way to reduce the carbon footprint of the process.

**A Promising New Cement – Solidia Technologies**

In the context of possible avenues to reduce limestone usage, a low lime containing non-hydraulic cement that cures into concrete in a $CO_2$/water environment has been recently introduced under a process patented by Solidia Technologies[1]. In that approach, about 5% of the resulting concrete mass is sequestered $CO_2$ [6]. The result is a silica and calcium carbonate bonding matrix that can be designed to provide compressive strength, abrasion resistance and freeze-thaw cycling resilience. Solidia Cement™ (SC) is a Calcium Silicate Based Cement and requires less limestone than OPC. In addition, the heat energy requirements in the kiln are lower, thus reducing the $CO_2$ emissions up to an additional 30%.

[1] Solidia Cement™ is a registered trademark of Solidia Technologies

It reduces the $CO_2$ footprint associated with the manufacturing and use of cement (the use being in concrete) by 70%, as shown in Figure 1.

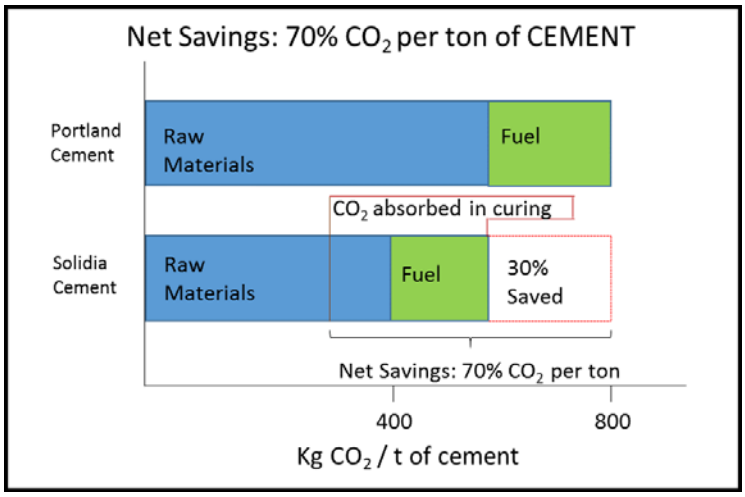


Figure 1: Net Savings in Carbon Dioxide Emissions with SC- based Concrete. Adapted from [6].

Considering that ~5% of the $CO_2$ emissions come from the cement industry along with the fact that the global $CO_2$ emissions are in the order of ~30 Gtons, the use of an alternative green concrete can have a considerable impact on the greenhouse gas emissions reduction that could conceivably be in the order of ~0.5 Gtons (considering only the cement making process) if all cement manufacturers worldwide adopted that process. Moreover, in the context of improving environmental sustainability, Solidia Concrete™, [2] (SC-concrete) contributes not only in reducing the carbon footprint from the concrete making process, in addition, the process uses a significant lower amount of water. Same as with OPC, the concrete assemblies made with SC-concrete require water for forming and shaping. Inversely, the water used in the concrete formulations based on SC is not consumed chemically, therefore it can be recovered during the curing process with carbon dioxide.

[2] Solidia Concrete™ is a registered trademark of Solidia Technologies

On average, ~75% of the water used in the developmental variation of the SC-concrete formulation can be recovered. If SC-concrete were used as an alternative to PC based concrete, the annual global water savings could approach approximately 2 billion tons, or two trillion liters [7].

**The Reinforcement Corrosion Control Challenge**

Reinforced concrete structures are expected to have a long service life with minimal maintenance. Corrosion of reinforcing steel is a major factor in reducing lifespan. Corrosion products occupy a larger volume than that of the consumed steel, generating tensile stresses that crack the concrete cover [8, 9]. Corrosion control in OPC concrete is well established because the pore water pH of the PC based concrete is alkaline (pH ~13). Thus, the reinforcement develops a passive layer that extends the service life of the structure considerably. However, conditions for SC-concrete are different. In this material cured by carbonation, the pore water has a significantly lower pore water pH (e.g., 9) than that of OPC, making it more difficult to retain a stable passive film on the steel. Thus, the structure is more vulnerable to corrosion damage from the early stages of exposure. However, several factors beyond pore water pH also influence the corrosion behavior in reinforced concrete structures. Properties of the new material, such as high electric resistivity, may be important factors in mitigating corrosion. Moreover, rebar corrosion resistance may vary with surface treatment or improve with the use of protective coatings. Information on the resulting corrosion conditions is needed and addressed by this work.

**Objective**

The research described in this thesis seeks to provide an initial assessment of the corrosion performance of plain and alternative reinforcing steels embedded in a developmental version of SC-concrete.

The assessment is intended to aid in determining the feasibility and potential use of this material for construction purposes when the structures are exposed to specific service regimes relevant to the expected deployment environment.

**Approach**

- Test reinforced SC-concrete specimens containing plain steel rebars with various surface finishes and a protective coating, and exposure to environments spanning a wide range of corrosion severity
- Test will be conducted in environments simulating both sheltered indoor and chloride-free outdoor regimes (expected initial deployment service applications for the developmental variation of SC-concrete). Salt water exposure tested as an extreme regime control
- Determine corrosion rates and evolution under the various environmental conditions evaluated
- Determine material properties that may impact corrosion performance

## CHAPTER 2: REVIEW OF FUNDAMENTALS

### Corrosion

Corrosion is defined as the deterioration of a metal because of reaction with its environment [8]. When a material is being selected for structural, engineering or architectural applications, corrosion resistance always has an important role to play. Moreover, when discussing the corrosion resistance of a material, the rate of corrosion is one of the primary factors to be determined.

### Electrochemical Considerations

When corrosion occurs, the corroding material loses at least one electron, while a chemical specie in the surrounding environment consumes them. This is called a redox reaction; in this reaction, the species losing the electron is being "oxidized" and the other species that gains the electrons is being "reduced". Equation 2 shows the reaction between iron (Fe) and oxygen ($O_2$), where iron (Fe) is the element being oxidized and oxygen ($O_2$) is being reduced. If the oxidized reaction or reduction reaction are considered individually, they are regarded as a half-reaction. This is better illustrated in Equation 3 and Equation 4

$$2Fe + 2H_2O + O_2 \rightarrow 2Fe^{2+} + 4OH^- \rightarrow 2Fe(OH)_2 \quad (2)$$

$$Fe \rightarrow Fe^{2+} + 2e \quad (3)$$

$$O_2 + 2H_2O + 4e \rightarrow 4OH^- \quad (4)$$

For corrosion to occur, four components have to be present:

- Anode: The location where the species will be oxidized
- Cathode: The location where the species will be reduced

- Electrolyte: Ionized solution
- Electronic pathway: Path that allows electron transfer

When a system is at equilibrium, there is no net chemical reaction. This point of equilibrium is associated with an equilibrium potential, which by convention is zero "0". If this equilibrium potential is changed, there would be current flow, and the system would be polarized.

Some otherwise highly reactive metals such as iron, chromium, nickel and titanium lose chemical reactivity under certain environmental conditions [8, 10]. This property of some materials is known as passivity, resulting from the formation of a protective surface film. In the case of iron, within a certain range of potential and at certain range of pH (typically alkaline), the iron develops a very thin (e.g., 3 nm) layer of protective oxide, and corrosion under these conditions is extremely slow. This is the case for reinforced OPC concrete, where the pore water pH is ~13 for which the passive film is stable. Consequently, corrosion is not severe until the passive layer breaks down. When this occurs, the metal goes into the active state. This passivity break down can occur by the action of external agents.

**Corrosion of Steel in Concrete**

Reinforcing steel bars are placed in concrete to provide resistance to tensile stresses [11]. OPC based concrete is characterized by alkaline pore water (pH ~13) causing the rebar surface to passivate. Nevertheless, depassivation of the metal can occur due to the penetration of chloride ions from the environment into the concrete and/or by interaction of the pore water of the concrete with carbon dioxide which can lower the pore water pH causing the metal to depassivate. According to Tuutti's model for steel corrosion sequence in concrete (see Figure 2) [12], the phase where this aggressive agents start penetrating the concrete cover until a

determined threshold value it is reached and corrosion begins, is known as initiation stage. Then, the propagation stage will take place and several factors such as resistivity of the concrete, porosity and moisture content of the pore water in the concrete, will influence the rate at which corrosion occurs.

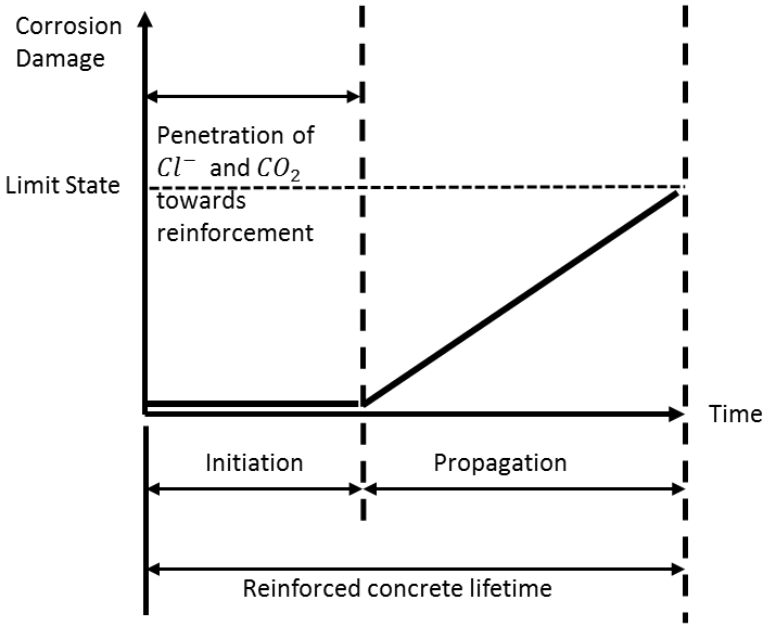


Figure 2: Schematic for Steel Corrosion Sequence in Concrete. Adapted from [12]

Once the corrosion process has initiated, the iron dissolution (anodic reaction) and oxygen reduction (cathodic reaction) will start to take place, this is known as the propagation period. In reinforcing concrete undergoing corrosion, the electrolyte will be the water in the pore network and the electronic pathway would be the rebar.

Corrosion products occupy a larger volume than that of the consumed steel, generating tensile stresses that crack the concrete cover [8, 9] when a given amount of corrosion has been reached. The resulting damage increases with time until it reaches a limit state that could make the structure unserviceable (serviceability limit state) or even seriously affecting structural

integrity (ultimate limit state) [13]. When the limit state is reached, the nominal service life of the structure and the end of the propagation stage have both been reached as well.

Thus, when considering an alternative to OPC based concrete, is important to assess the corrosion performance of the new material and have an understanding of the concrete properties that may have an impact in such corrosion performance and of the resulting corrosion rates.

Some of the concrete properties valuable for understanding corrosion behavior are:

- Porosity: Porosity of the concrete is an important parameter that can impact mechanical behavior and transport properties. Transport properties are intimately related to various durability problems [14]. From a corrosion standpoint, porosity affects the mobility of water and substances around the steel [12]. Initially when concrete is exposed to water, the concrete will start to absorb it. This is known as capillary sorption. Thus, the pore network represents a pathway for potential aggressive agents to reach the reinforcement and initiate a degradation process. Moreover, this matrix can affect the oxygen diffusivity through the concrete cover
- Resistivity: Electrical resistivity is an indication of the combined effect of the amount of moisture in the pores, the size and tortuosity of the pore system, and the resistivity of the pore solution itself [15]. Concrete with high resistivity could retard the corrosion process by restricting the efficiency of the electrolytic pathway between anodic and cathodic regions. Moisture Content: Moisture content is a measure of the amount of electrolyte in the pore system [12]. Moisture has an effect in the initiation time for reinforcing corrosion. It can provide a faster pathway for chloride ion penetration (which happens through the liquid phase). In the propagation stage, moisture has an influence in the corrosion rate; intermediate moisture conditions provide access of oxygen giving as well

an electrolytic pathway between anodic and cathodic regions. [16] However, very high moisture content can impede oxygen access by blocking the oxygen transport pathway that would have existed through the unfilled portion of the pores, and actually lower the corrosion rate as a result. At the other extreme, very low moisture would allow fast oxygen access, but with very limited electrolyte transport thus also lowering corrosion rates.

- Pore Water pH: It has been determined that the pH of the pore water has an influence on the passivation of a material and is a useful property to better understand its behavior from a corrosion standpoint. The Pourbaix diagram, is a map that shows the regimes of stability of the passive film layer as a function of the potential and pH of the surrounding environment. Therefore, they are frequently used to predict the effect of pore water pH in the system. For PC based reinforced concrete, the pH is ~13 and for this pH value, iron shows passive behavior in a range of potential between -0.2 and 0.2 V vs the standard hydrogen electrode at 25C [17] meaning that, under these conditions, corrosion is very slow.

**Techniques for Establishing Corrosion Performance Addressed by this Work**

- Open Circuit Potential (OCP)

A rebar embedded in concrete reaches a mixed potential against a reference electrode. This potential is a result of the interactions between the iron oxidation and oxygen reduction. When corrosion initiates, the dissolution of iron is faster and the potential would shift toward more negative values, when this shift occurs the system will be activated [11]. Therefore, the open circuit potential measurement serves as an indication of the probability of corrosion, or

corrosion state of the system. The open circuit potential measurements do not represent an indication of the corrosion rate of the system.

- Electrochemical impedance spectroscopy (EIS)

This technique consists on slightly changing the electric potential of the steel (typically less than 10 mV) at a predetermined frequency by means of an electric oscilator connected the steel (working electrode) and to a counter electrode to complete the circuit through the concrete. The voltage is controlled by an automatic potentiostat. Afterwards, the voltage and current are recorded as a function of frequency. Measurements of the amplitude and phase angle of the excitation current and the potential response are made over a wide range of frequencies that usually go from 1 mHz to 1kHz. Each frequency would define the complex vector electrochemical impedance "Z", determined by the ratio of the potential response phasor (V) to the excitation current density phasor (i) [18]. Therefore, the measurements at different frequencies can be represented by a group of points in a complex plane. This is known as the Nyquist diagram.

When the system has a simple behavior, there is a relationship between the corrosion current Icorr and the polarization resistance Rp given by the deviation of potential of the system and current response.

$$Icorr = {}^{B}/_{Rp} \tag{6}$$

Icorr = Corrosion current

B = Stern-Geary Constant determined by the kinetic properties of the system (approximate value of 0.026 V for steel in concrete) [18]

Rp = Polarization resistance

Once Icorr has been established, the current density icorr is determined by dividing Icorr over the steel area exposed in the concrete (for the specimens evaluated in this Thesis is equivalent to 40cm$^2$). Finally, the corrosion rate C.R can be obtained by means of the following equation [19]:

$$C.R. = icorr * K \quad (7)$$

C.R = Corrosion rate (um / y)

icorr = Corrosion density (μA / cm$^2$)

K = Penetration rate equivalent constant (for iron = 11.68 (um/y)/(uA/cm$^2$) [19]

However, the measurement of the polarization resistance "Rp" is often affected by the interfacial capacitance of the steel "Cdl" in parallel with Rp. Moreover, the electrolyte resistance "Rs" of the concrete is between the point where the potential is measured (reference electrode) and the surface of the steel. The system to be evaluated can then be considered in terms of a simplified equivalent circuit as the one shown in Figure 3. Moreover, the interfacial capacitance is often a non-ideal component requiring additional consideration during analysis of the results.

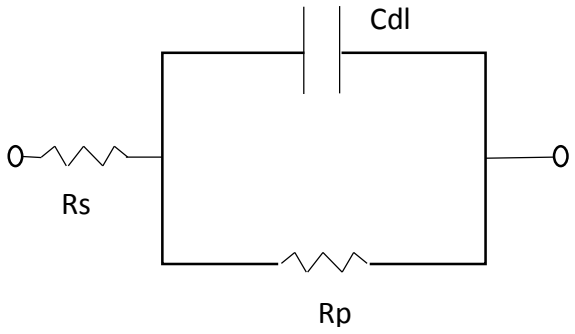


Figure 3: Equivalent Circuit for the System under Consideration

The theory of alternating current establishes that a circuit of this type would have a Nyquist diagram similar to the one in Figure 4. Therefore, by means of electrochemical impedance spectroscopy it is possible to establish the corrosion rate of the system through Rp and estimate the concrete resistivity through Rs. Typically, the Rp of the system can be found during the low frequency sweep, which is shown as a semicircle in the Nyquist diagram. In most cases, a full semicircle will not be present, but the data can be extrapolated to obtain Rp, and thus the apparent corrosion rate (ACR) of the system using Equation 6 and 7. Computer fitting of the results is usually made by means of commercially available software [20] to obtain an estimate of the value of Rp. That procedure was used to analyze the data obtained in this Thesis using the Echem Analyst software provided by Gamry Instruments, (Warminster, PA, US)

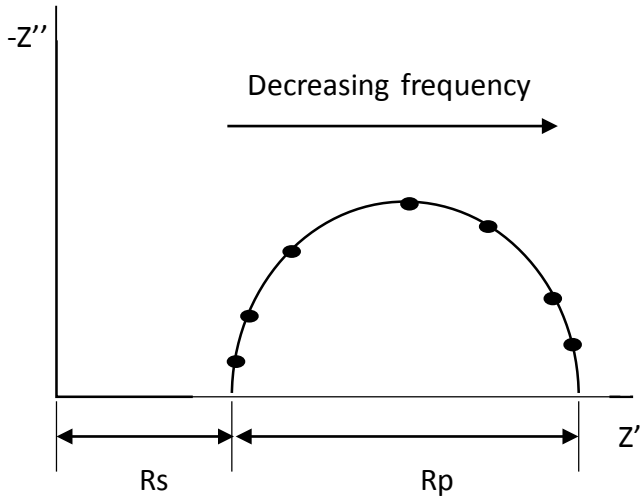


Figure 4: Nyquist Diagram

**Carbonation of Concrete Structures and Corrosion Rates**

In OPC based concrete, carbonation of the concrete by action of carbon dioxide in the solid and liquid phase leads mainly to the formation of calcium carbonate by reaction of the $CO_2$ with hydrated species within the concrete such as $Ca(OH)_2$. This process tends to be slow and it

affects some important properties of the concrete that, as previously discussed, have an effect on the corrosion initiation of the system.

The process of carbonation decreases the pore water pH of the concrete. Moreover, when carbonation reaches a specific depth, it can cause passivity break down and corrosion starts to take place. Several factors influence the rate of carbonation penetration such as: cement composition, porosity and relative humidity [21].

Table 1 presents a classification for different corrosion damage levels as a function of the corrosion rate based on the type of aggressive agent initiating corrosion and the moisture of the concrete [22, 23]:

Table 1: Risk of Damage for Reinforced Concrete in Relation to Corrosion Rates and Concrete Condition

| Risk of Damage | Range of CR uA/cm^2, (um/yr) | Condition |
|---|---|---|
| Very low | <0.1 (<1.17) | Very dry or carbonated concrete with no chloride contamination |
| Low | 0.1 - 0.5 (1.17-5.84) | Dry concrete, carbonated or with mild chloride contamination |
| Moderate | 0.5 - 1 (5.84 - 11.68) | Humid concrete, carbonated or with mild chloride contamination |
| High | 1 - 10 (11.68 - 116.8) | High humidity concrete, carbonation or affected by chloride attack |
| Very High | >10 (> 116.8) | High humidity and highly contaminated with chlorides |

In the case of concrete made with SC, the curing process is carried out with carbon dioxide. In this case, the material is carbonated from the beginning and without the presence of hydroxide species and alkali ions in the bonding matrix, a mildly alkaline environment is expected. This will make the formation of the passive layer on the rebar difficult. However, passivity of iron is not the only factor that affects the corrosion behavior of the system. Material

properties, such as porosity and resistivity, have an influence as well. Therefore, determination of such properties, along with the corrosion performance of the material are addressed by this work. In general, it may be thought that steel in SC-concrete could have corrosion performance that will relate to some extent to that of carbonated OPC concrete. This issue will be considered again later in the view of the experimental results.

**Microbial Induced Corrosion (MIC)**

The activity of certain living organisms can have an effect on the corrosion process of a system. Certain type of bacteria can have an influence in the rate of anodic and cathodic reactions that may enhance or in some cases retard the corrosion process [8]. In particular there are two species that have a significant impact on the corrosion process and durability of reinforced concrete particularly within wastewater environments or where the conditions for microbial growth are favored. Those are sulfate reducing bacteria (SRB) and sulfur oxidizing bacteria (SOB). SRB is a type of bacteria that under anaerobic conditions reduce sulfate ions to hydrogen sulfide.

Hydrogen sulfide tends to accelerate the metal dissolution. Moreover, if the hydrogen sulfide gas encounters with SOB which growth is prevalent in aerobic conditions and preferably low pH environments, sulfuric acid can be formed which in sufficient amounts could aggravate the corrosion process by decreasing the pH of the pore water within the concrete and promoting depassivation with consequent acid and sulfate attack [24]. There are other microorganisms that may indirectly have an influence in the corrosion rates of the system such as iron oxidizing bacteria (IOB) that at near neutral pH and typically microaerophilic conditions oxidizes ferrous ions to ferric ions.

This can lead to the formation of bulky iron oxides deposits that can enhance the corrosion rate of the system and reduce even more the life of a structure since the ferric oxides are more voluminous than ferrous oxides [25]. Moreover, the growth of iron bacteria can produce tubercles that promote crevice attack. Finally, chemoheterotrophic bacteria produce carbon dioxide that in typical OPC can produce carbonation, lowering the pH of the system, thus, enhancing the corrosion process.

The system conditions such as pH and oxygen concentration can favor or inhibit microbial catalysis for this processes to occur. For example, SRB typically grows in anoxic environment at pH near neutrality. Conversely, SOB is favored in aerobic conditions at low pH. While MIC is a well-documented mechanism of corrosion of the external surface of POC concrete itself, for example in sewers, MIC of the steel reinforcement inside the concrete has received little attention in the literature [26] possibly because the microorganisms that could be responsible for MIC may not encounter sufficiently favorable growth or nutrient conditions in the high pH pore water of OPC. The novel concrete examined here, compared to OPC may be in principle be more susceptible to MIC given the only mildly alkaline pH. This potential mechanism of induced corrosion should receive further study and consideration in the future.

# CHAPTER 3: METHODOLOGY

## Material Data

### *Surface Conditions of Reinforcement Bars*

The reinforcement bars used were supplied by GERDAU, Jacksonville, FL, US. Uncoated steel bars wre made of of plain carbon steel meeting ASTM A-615 [27] specifications. Epoxy-coated bars, also carbon steel, were supplied for the same source and met ASTM A-775 specifications [28] All bars were 0.5" (1.27 cm) in diameter (#4 rebar size). The bars were cut to segments of 6" (15.24 cm) in length. Three reinforcing bar (rebar) conditions were tested:

- Mill Scale "MS": This is ASTM A-615 rebar of the most common type used as reinforcement for concrete applications, and in its as-produced mill condition. Mill scale is the high temperature oxide layer formed during the manufacturing of the rebar.
- Sandblasted "SB": This material is used as reference for comparison with alternative coatings. The sandblasted rebars were made of normal production ASTM A-615 rebar that had the mill scale removed by using abrasive material blown against the surface at elevated pressure, leaving a bare metal surface.
- Epoxy coated with 0.25% surface breaks "EC": This widely available corrosion resistant material is prepared with rebar stock originally satisfying ASTM A-615 [27] specifications and then processed by sandblasting and coating with a 2-component powdered epoxy compound cured at elevated temperature. The intentional coating breaks were introduced by filing at regular intervals to obtain ~ 1mm$^2$ breaks to assess possible vulnerability in this medium.

***Concrete***

The concrete tested in these experiments was a proprietary variation of SC provided by Solidia Technologies®, Piscataway Township, NJ, United States. The manufacturing process of SC is similar to that of OPC, in fact it can be made in all plants designed to manufacture OPC. However, despite its similarities in the chemical raw materials and manufacturing process, they possess different profiles (Table 2). Conversely, SC cures in a $CO_2$/water environment and this process takes ~1 day. In the case of OPC based concrete, the curing process takes ~28 days and it is carried out with water.

Table 2: Relevant Properties of OPC vs SC. Adapted from [6]

| | **OPC** | **SC** |
|---|---|---|
| Basic Chemistry | $Ca_3SiO_5$ - $Ca_2SiO_4$ | $CaSiO_3$ |
| Raw Materials | | |
| Wt. % Limestone | 80% | 55% |
| Wt % Shale/Clay/Sand | 20% | 45% |
| Max. Kiln temp. | 1500˚C | 1200˚C |
| $CO_2$/t of cement | 800 Kg | 550 Kg |
| Energy/t of cement | 5.4 Gj | 3.8 Gj |

For experimental purposes, cylindrical specimens made with the developmental variation of SC-concrete were prepared and cured at the research facilities of Solidia Technologies. Twenty seven reinforced concrete specimens (nine for each type of rebar) and eleven plain concrete specimens that were part of an extended experimental matrix were used throughout the duration of the experiments addressed in this Thesis. The concrete portions of all the specimens measured 3” (7.62 cm) in diameter and 6” (15.24 cm) in length. The reinforced and plain concrete specimens are shown in Figure 5.

Figure 6 shows a detailed schematic and dimensions for a reinforced concrete specimen. For non-EC specimens, a 1 inch long region around the level where the rebar emerges from the concrete was covered with a layer of two-component epoxy to avoid corrosion at that interface, which would not have been representative of the behavior of interest.

Figure 5: A Batch of Reinforced and Plain Concrete Specimens that Includes those Addressed in this Thesis.

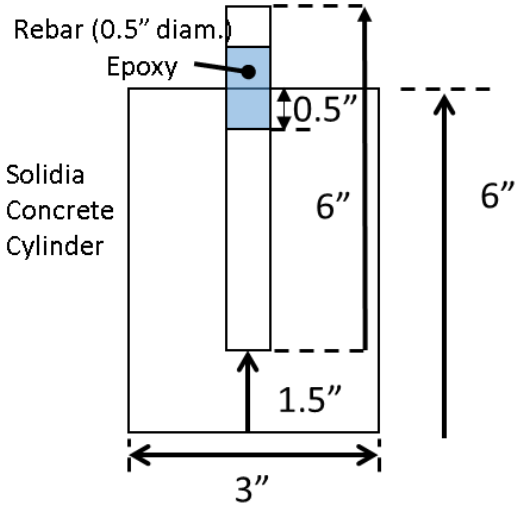


Figure 6: Schematic of a Reinforced Concrete Specimen

**Experimental Setup: Exposure Regimes**

The following exposure regimes were selected for evaluation with the indicated rationale:

- Atmospheric environment with 85% relative humidity: Simulating indoor service
- Partial submersion in distilled water (FW) : Simulating outdoor chloride – free service
- Partial submersion in mildly corrosive water (MW): 100 ppm of chloride ions introduced as sodium chloride (NaCl) and 200 ppm of sulfate ions introduced as sodium sulfate ($Na_2SO_4$). Simulating an environment slightly more aggressive than fresh water, representative of conditions that are sometimes considered to be representative of the boundary between acceptable and unacceptable service severity [29].
- Partial submersion in salt water water (SW) : The salt water was prepared with distilled water with 5% w/w (NaCl). Salt water simulating extremely aggressive marine conditions as a bounding case. The Cl- ion content, about 1 M, was intended to be somewhat more aggressive than that encountered in natural sea water regimes [30], but for simplicity no other major ions were incorporated in this medium.

A schematic of a reinforced specimen exposed to an immersion regime Figure 7. All tests were performed in triplicate and at laboratory/ambient temperature (~25 +/- 3˚C). For the immersion regimes, the tests were accelerated via partial immersion considering a worst case scenario. Partial immersion is a highly aggressive condition with the following characteristics [16]:

- Promotes species entry via fast sorption
- Evaporative concentration near waterline
- Strong electrolyte presence in lower part of specimen
- Fast oxygen access in upper part (part not submerged)

- Promotes formation of active corrosion macrocell
- Rapid evolution towards a corrosion propagation mode

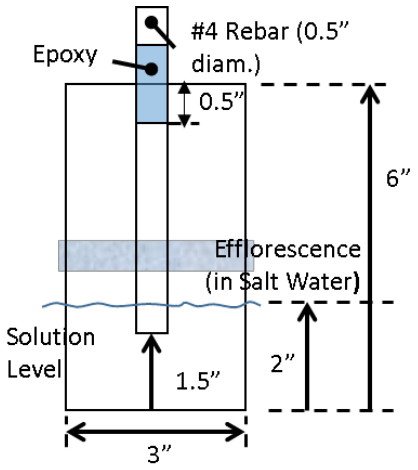


Figure 7: Schematic of Reinforced Specimen Exposed to an Immersion Regime

**Experimental Setup of Immersion Regimes**

The specimens were placed in a plastic tray of 15.5" (39.37 cm) by 16.5" (41.91 cm) holding a number of specimens that included those used in this study (triplicate specimens of each type of reinforcement condition). The fresh water, mild water and salt water solutions were prepared accordingly to the specifications mentioned above and the specimens were submerged to cover 2" (5.08 cm) in length of the specimens. An MC DAQ data acquisition system was used to measure the open circuit potential for each specimen as to be used as one metric for determining whether corrosion is taking place.

For this purpose, each tray had an activated titanium electrode [31] that served as a reference electrode; each specimen was identified, connected and programmed into the data logger. Therefore, the electric potentials could be monitored in real time and the data could be easily collected for further analysis; Figure 8 shows a schematic of the specimens under immersion conditions. For comparative purposes, regular calibrations of the activated titanium reference electrodes versus a saturated calomel electrode (SCE) were performed. The saturated

calomel electrode was chosen because of its common usage as an electrochemical reference. However, the use of titanium reference electrodes in this case was imperative because they are generally less affected by prolonged contact with the solution and thus more suitable for long term analysis of the specimens on immersed regimes.

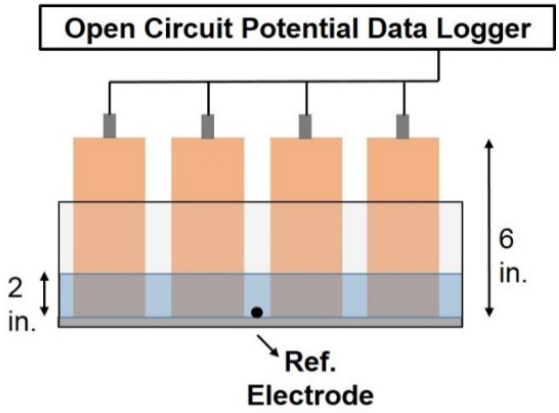


Figure 8: Schematic of the Specimens Placed in the Tray and Connected to a Data Logger

Figure 9 shows the appearance after ~3 months of the specimens exposed to mild water and Figure 10 shows the appearance after ~3 months of the specimens exposed to salt water. Notice in this case the efflorescence or ring of salt, a phenomena that consists of deposited salts that are leached out of the concrete and are crystalized on subsequent evaporation of the water or interaction with carbon dioxide from the atmosphere [3]. This efflorescence can be seen on the specimens exposed to salt water in Figure 10.

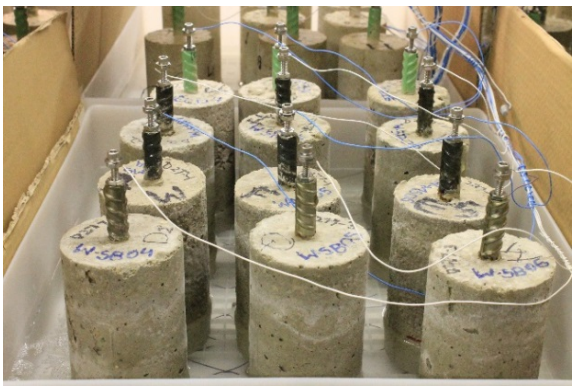

Figure 9: Batch of Specimens Exposed to Mild Water that Includes those Evaluated in this Thesis

Figure 10: Batch of Specimens Exposed to Salt Water that Includes those Evaluated in this Thesis

***Conductivity of the Solutions***

Is expected that the level of water in the trays will diminish progressively as the trays are exposed to the atmosphere due to evaporation. To compensate, fresh distilled water was added to the trays to maintain the specimens 2" (5.08 cm) depth of submersion. However, the constant addition of distilled water along with frequent mobilization of the specimens into and out of the trays for further examination eventually led to the dilution of the mild and salt water solutions, thus decreasing the conductivity of the solutions. When this occurred, the addition of an appropriate amount of the respective ionic solutions to the trays instead of fresh water was the next step.

To further monitor the conductivity, resistance of the solution was measured using a Nilsson meter and a probe with known length and cross sectional area. The experimental setup is on Figure 11. Once all the connections were made, the probe was cured with distilled water and then fully submerged in the tray where the solution conductivity was going to be determined (without disturbing the concrete specimens in the tray). The resistance was detected and properly recorded along with the temperature of the solution in the tray. Finally, the probe was carefully washed with distilled water before proper storage.

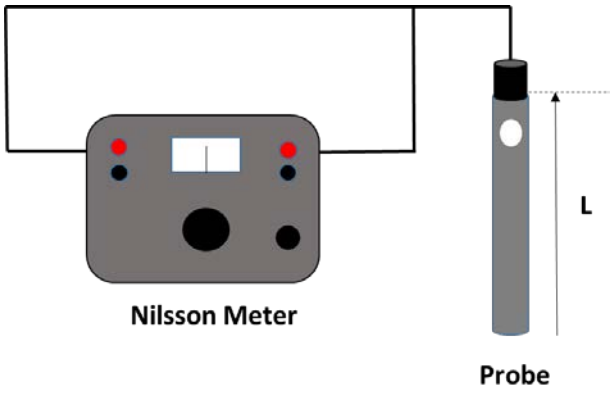


Figure 11: Experimental Setup for Conductivity Measurements

With all the gathered data, the resistance was converted to resistivity and conductivity according to the following mathematical equations.

$$R = \frac{\rho L}{A} \tag{8}$$

where:

R = resistance (ohm)

ρ = resistivity (ohm·cm)

L = length of the probe (cm)

A = cross sectional area of the probe ($cm^2$)

Finally, the conductivity σ (mS/cm) is the inverse of the resistivity, ρ.

$$\sigma = \frac{1}{\rho} \tag{9}$$

Since the conductivity changes with temperature, all the results were temperature corrected to 22˚C following Equation 10 [32].

$$\sigma_2 = \frac{\sigma_1}{1 + TC * (T_1 - T_2)} \tag{10}$$

where:

$\sigma_2$ = New conductivity value corrected to a fixed temperature (mS/cm)

$\sigma_1$ = Conductivity obtained at the experimental temperature (mS/cm)

TC = Temperature coefficient of inorganic electrolytes at 18˚C (mS/cm - ˚C)

$T_1$ = Temperature recorded during the experiment (˚C)

$T_2$ = Fixed temperature (˚C)

Figure 12 illustrates the conductivity values for the solutions throughout the course of the experiments. These values are consistent with expected values based on solution composition.

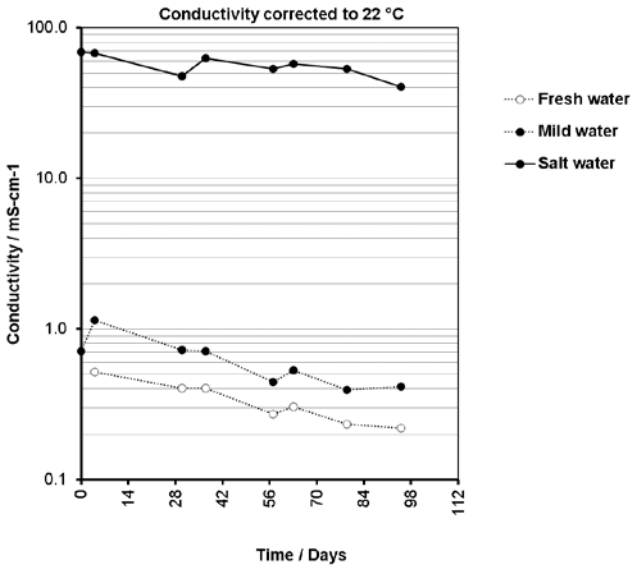


Figure 12: Conductivity of the Solutions used for the Exposure Regimes

***Electrochemical Impedance Spectroscopy (EIS)***

Electrochemical impedance spectroscopy is one of the most common techniques to estimate corrosion rates of a system. A Gamry Instruments, Model Reference 600 potentiostat/galvanostat/ZRA (Warminster, PA, US) was used for this purpose. The specimens were tested in the frequency range of 100 kHz to 0.1 mHz with a 10 mV r.m.s. excitation amplitude. A schematic of the cell is shown in Figure 13.

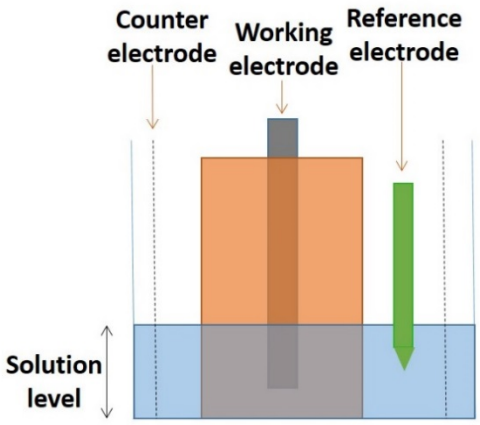


Figure 13: EIS Test Cell for Immersion Regimes

Components of the EIS test cell for immersion regimes

- Reinforcing bar as working electrode
- Activated titanium counter electrode
- Saturated calomel reference electrode (SCE)
- Test solution and solution level same as that in tray
- After testing, specimens returned to the correspondent exposure tray

***Concrete Resistivity***

The resistivity of the concrete was estimated from the electrochemical impedance spectroscopy tests, assuming that the a.c. potential between the rebar and the surface of the concrete varies only radially and in the immersed zone for simplicity (Figure 14). Thus, Equation (11) applies [33].

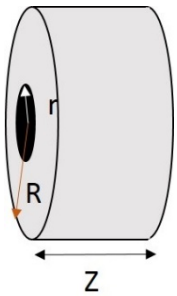


Figure 14: Schematic of Immersed Zone of the Concrete Specimen

$$\rho = \frac{R_s * 2\pi * Z}{\ln(\frac{R}{r})} \quad (11)$$

where:

Rs = solution resistance (obtained by EIS) ohm

ρ = concrete resistivity (ohm·cm)

Z = length of the bar (cm)

R = diameter of the specimen (cm)

r = diameter of the rebar (cm)

Finally, it was assumed that the rebar extends fully to the bottom of the specimen. This simplified abstraction is illustrated in Figure 15.

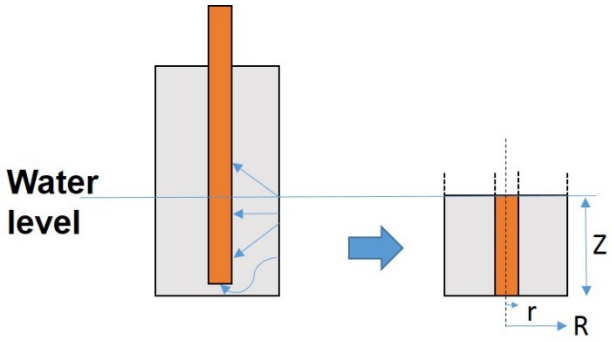


Figure 15: Abstraction for Immersion Regimes (Concrete Resistivity).

**Experimental Setup of Atmospheric Regime**

For the atmospheric regime, three specimens for each type of reinforcement were placed in a chamber with 85% relative humidity (RH). Saturated Potassium Chloride KCl was used to replicate this relative humidity condition in the closed environment [34]. To determine the relative humidity of the environment a hygrometer from Taylor Precision Products Inc. (Rochester, NY, USA) was used. Figure 16 shows the specimens placed in this exposure regime.

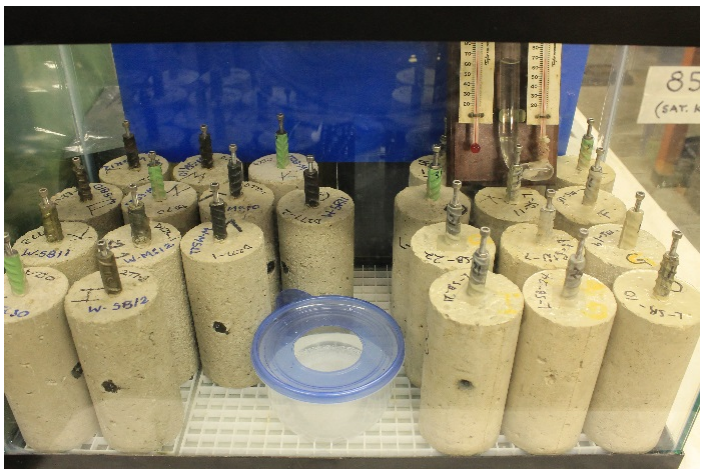

Figure 16: Batch of Specimens Exposed to 85% Relative Humidity that Includes those Evaluated in this Thesis

***Open Circuit Potential Measurements***

The specimens exposed to 85% relative humidity were regularly taken out of the chamber for potential measurements. An MCM meter LC-4 from M.C. Miller Co., Inc. (Ringwood, NJ, USA) was used for this purpose along with a SCE. A schematic of the system is on Figure 17. A humid sponge was placed against the bottom of the SCE for better contact with the specimen. The open circuit potential of the rebar was then measured using the SCE as reference.

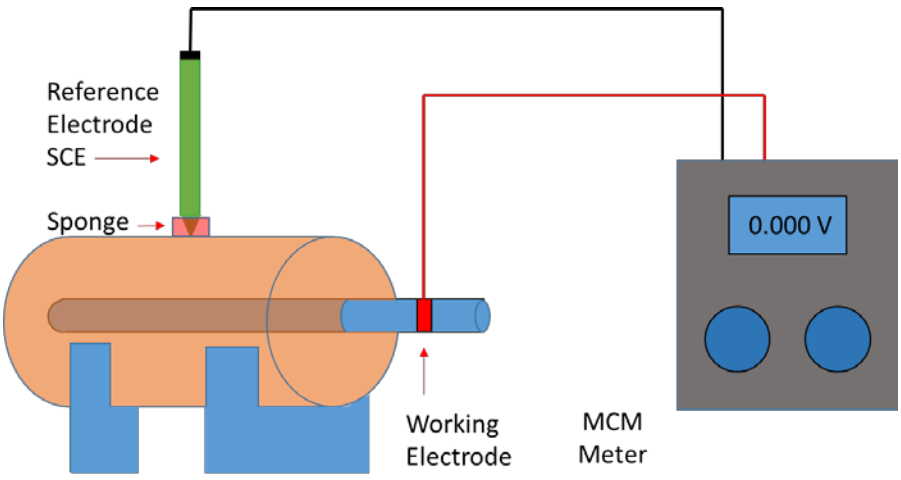


Figure 17: Schematic of Potential Measurements for Specimens in 85% RH

***Electrochemical Impedance Spectroscopy***

This technique was used following the same premises and parameters as those of the immersion regimes. Comparable to the procedure for the immersed specimens, the Gamry Instruments, Reference 600 potentiostat/galvanostat/ZRA (Warminster, PA, US) was used and the specimens were tested in a range of 100 kHz to 0.1 mHz with a 10 mV r.m.s. excitation amplitude. A schematic of the cell is shown in the Figure 18.

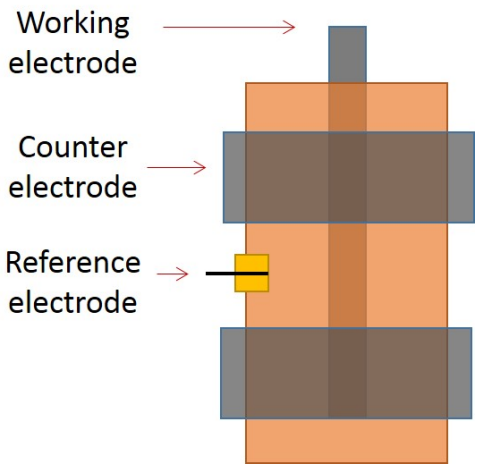


Figure 18: EIS Cell for 85% RH Regime

Components of the EIS test cell for immersion regimes

- Reinforcing bar as the working electrode
- Clamped conductive rubber ring dual counter electrode, does not alter humidity condition of concrete.
- Activated titanium reference electrode embedded in grout near surface
- Specimens tested temporarily outside chamber, placed in a chamber that replicates the humidity conditions to reduce drying in lab air
- After testing, specimens returned to 85% RH chamber

***Concrete Resistivity***

For determining the concrete resistivity of the specimens exposed to 85% relative humidity, the same procedure as to that of immersed regimes was followed using Equation 11. However, in this case, roughly the total length $Z_t$ (Figure 19) of the specimen was exposed to the environment, hence it was used as Z for the calculations. For simplicity, it was assumed that the rebar extended to the bottom of the specimen.

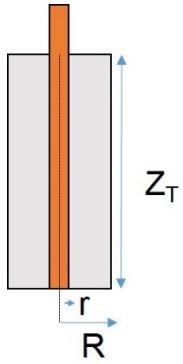


Figure 19: Simplified Schematic of Specimen Exposed to 85% RH for Resistivity Calculation

**Experimental Procedure: Other Material Properties**

***Material Properties: Volumetric Porosity***

The volumetric porosity of a material is given by equation 12

$$\% \, Porosity = \frac{Vvoids}{Vconcrete} \tag{12}$$

Three plain concrete specimens with 3” diameter and 6” length in the as-received were selected for this experiment. Initially they were submerged in water to half their length (3”; 7.62 cm) in a closed chamber (to maintain 100% relative humidity). The amount of water uptake was continuously monitored by weighting the specimens on a 0.1 g precision digital balance. After approximately one week of exposure, the specimens were taken to full immersion and they were

frequently weighted until there was no more mass gain and the levels were stabilized. With that data, the part of the porosity that was not filled in the as-received conditions was calculated, taking into account that the volume of the voids per $cm^3$ will be equivalent to the maximum mass of water in grams that the specimen gained, at the particular moment when stabilization is reached, assuming that all the pores within the concrete are completely filled with water. The volume of the 3" (7.62 cm) by 6" (15.24 cm) concrete specimens is 695 $cm^3$.

To obtain an indication of the total volumetric porosity of the material it was necessary also to obtain the evaporable amount of water of the as-received specimens. For this, another three plain concrete specimens of 3" (7.62 cm) diameter and 6" (15.24 cm) length were used. Their as-received weight was recorded and following ASTM C642 [35] specifications for oven-dry mass determination, they were placed in a Thelco GCA/Precision Scientific oven at 104˚C for a time greater than 24 hours. Afterwards, the specimens were placed in a desiccator for ~1 hour and then, the mass was measured. The process was repeated until the difference in the last two mass measurements was lesser than 0.5%. With this information, the volume of the voids that were filled with water in the as-received material was determined and added to the volume of the voids that were not filled with water in the as-received condition (obtained from the other set of 3 specimens) to estimate the total volumetric porosity.

***Material Properties: Weight Gain in Test Media***

An important property that was assessed over the course of the experiment, is related to the weight that the reinforced concrete specimen gains when it is exposed to a certain environment. This is indicative of extent/speed of capillary absorption of the material. Therefore, it is an important parameter from a corrosion initiation standpoint.

Three specimens for each immersed exposure condition (one for each type of reinforcement) were randomly selected for monitoring. In the case of the 85% RH exposure, all the specimens were monitored. All the selected specimens were regularly weighted for this purpose. For the immersion regimes, the excess of water was gently dried with paper towels before weighing every time. A 0.1 g precision digital balance was used.

***Material Properties: Native Internal Humidity***

To determine the native humidity of the concrete, eight plain concrete specimens of 3" (7.62 cm) diameter, 6" (15.24 cm) length were randomly selected. To establish the internal humidity, duplicate specimens were exposed to four different relative humidity conditions and their mass gain or loss was monitored frequently using a 0.1 g precision analytical balance. With the gathered data, the internal relative humidity of the material can then be estimated. The environments selected for the experiment are the following:

- 62% relative humidity**:** laboratory exposure, (RH confirmed with a hygrometer from Taylor Precision Products Inc. (Rochester, NY, USA))
- 75% relative humidity: A closed chamber with a saturated solution of sodium chloride NaCl provided this condition.
- 85% relative humidity: A closed chamber with a saturated solution of potassium chloride KCl provided this condition.
- 100% relative humidity: A closed chamber with fresh water that was not in direct contact with the specimens was used for this purpose.

In addition, data gathered for the weight gain evolution of reinforced concrete specimens exposed to 85% RH was included for the analysis since it was readily available and provided another point to support the results obtained.

During the course of the experiments it was found that the mass was changing approximately with the square root of time, as it is seen often in diffusion controlled processes [36]; Thus, the behavior was assumed to be taking place according to the following equation:

$$m = K * \sqrt{t} \tag{13}$$

For each environment considered, K can be determined as the slope obtained by plotting the change of mass as function of time and fitting the results via a least square error trend line according to Equation 13. With that information, the native moisture can be determined as the point where K is equal to zero implicating that the specimen is in equilibrium with the surrounding environment and neither gains or loses weight. This can be easily determined by plotting the K average values for each environmental condition and interpolating for the value where K equals zero.

***Material Properties: Pore Water pH***

Two plain concrete specimens with 3" diameter and 6" length were selected for this experiment. The in-situ leaching method for pH determination was followed [21]. For this, the specimens were placed in a 100% RH environment and allowed to stabilize for one month. After that, three holes were drilled into the upper part of the specimens using a hammer drill with a 1/16 in. (0.16 cm) masonry drill bit with 3 cm of separation from each other, as can be seen in Figure 20. Afterwards, an acrylic washer was placed on top of the holes, fixed with fast drying epoxy and the hole was closed with a rubber cap.

The holes were filled with distilled water up to the bottom of the plastic washer, returned to the 100% RH chamber and monitored periodically for absorption loss into the surrounding concrete, the water added equilibrated with the water in the pore network, meaning there was no

more water loss due to absorption into the surrounding concrete. In this specific case, the stabilization was achieved after ~10 days.

The pore water pH was determined by detecting the potential difference between the reference and sensing electrode when immersed in the pore water solution with a pH meter model 140 from Corning Inc (Corning, NY, USA); using an activated Titanium microelectrode and a silver-silver chloride (SSC) reference electrode at laboratory temperature (~25 +/- 3 °C).

Initially a calibration curve was made with buffered solutions for pH 7, 8, 9 and 10 to be able to determine the range of potential of the pore water. Afterwards, the measurements were conducted by introducing the reference electrode into the reference hole and the glass electrode into either hole 1 or 2 (see Figure 20), both electrodes were submerged for 30 seconds and the potential measurement was recorded. The procedure was repeated with buffered solutions of pH 8 and pH 9 or pH 9 and 10 accordingly.

The measurements were done by triplicate in the 4 testing holes (two for each specimen). Finally, the potential readings were converted to pH values using linear potential interpolation/extrapolation from the calibration points.

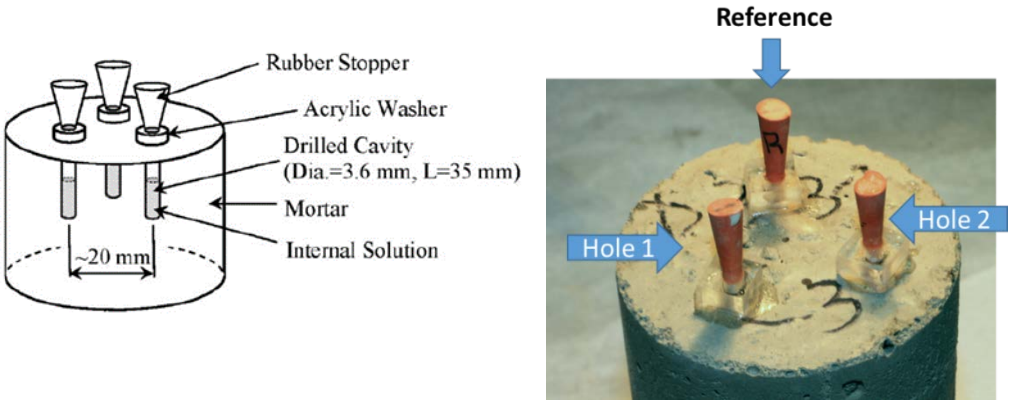


Figure 20: Schematic of ISL Experimental Setup and Example of Specimen Evaluated in This Thesis. Source: Sagüés et. al. [21]

# CHAPTER 4: RESULTS AND DISCUSSION

## Evaluation Period

Test exposures were successfully conducted over a period of ~170 days. While that period is short compared with the expected service life of most components in actual applications, the early information obtained in this investigation nevertheless provided important insight on the corrosion performance of steel in the developmental variation of SC-concrete examined here. Additional monitoring for a longer period is anticipated in follow up work.

## Potential Measurements

Potential measurements are shown in Figures 21-24. For the 85% RH atmospheric exposure there was indication of generally passive behavior (no potential drop), for all rebar surface conditions examined over the entire test period.

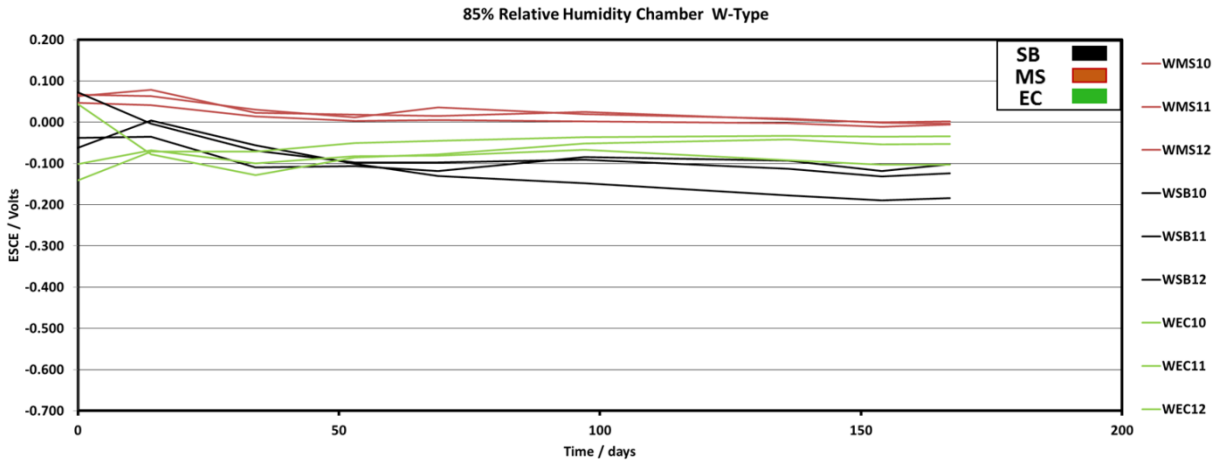


Figure 21: Potentials of Specimens Exposed to 85% RH

For the three immersion regimes, all rebar surface conditions showed a potential drop indicative of early activation (typically after ~1 week of exposure). Notice that for EC rebar, activation took place on the very small coating break zones. Differentiation in activation times between surface conditions was small in absolute terms in the context of the overall test duration. EC rebar behavior, shifting to more positive potentials later on likely reflects lower probability of stable activation due to the very small (0.25%) fraction of exposed metal.

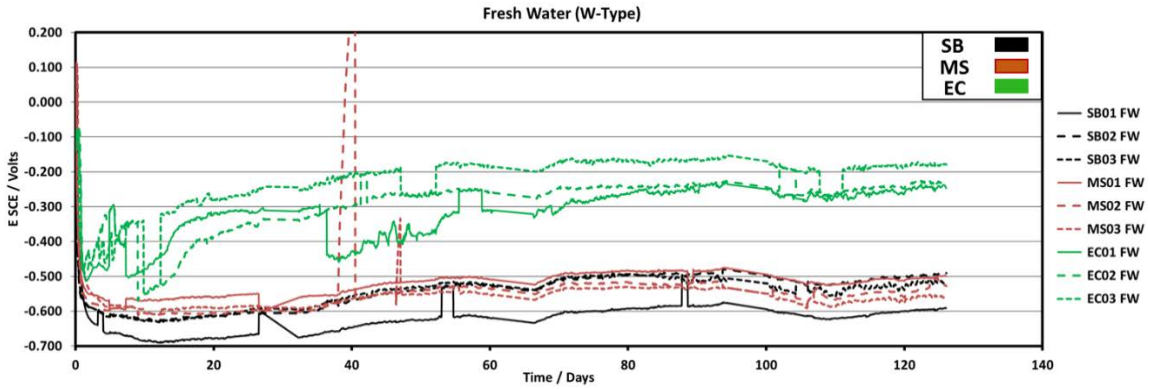


Figure 22: Potentials of Specimens Exposed to Fresh Water

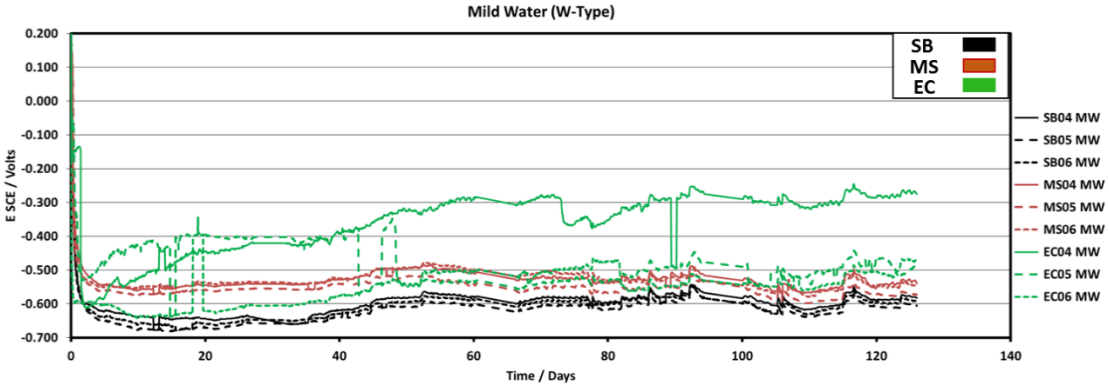


Figure 23: Potentials of Specimens Exposed to Mild Water

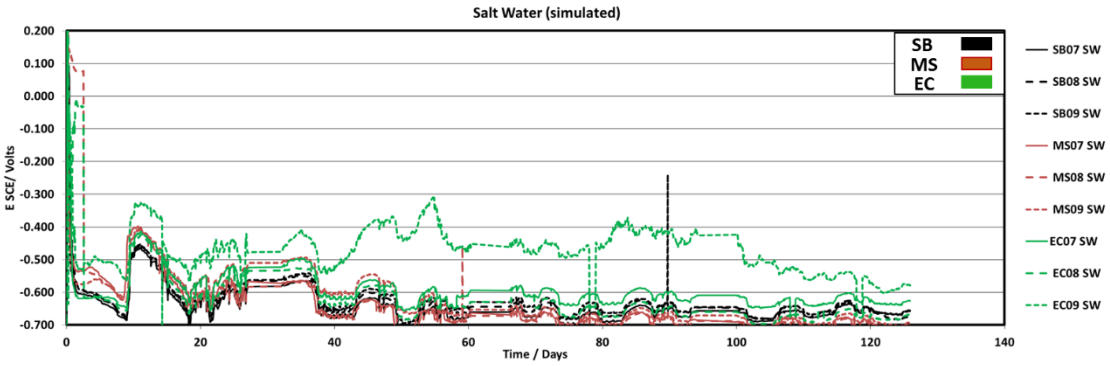


Figure 24: Potentials of Specimens Exposed to Salt Water

**EIS Results and Apparent Corrosion Rates over Time**

Figures 25 and 26 show examples of typical EIS behavior for specimens with high and low values of ACR respectively. The results are shown in both Nyquist and Bode [18] format, and present a number of commonly encountered complications [11] above those of the highly simplified diagram that was shown in Figure 4. A high frequency semicircle that is sometimes visible is related to the concrete dielectric properties and not to the corrosion rate. The polarization resistance Rp was estimated, as shown in Figure 26, by fitting to a basic nominal Rs (not always the same as that used for resistivity measurements) in series with Rp/CPE parallel combination model fitting with the software package indicated earlier; the lowest two frequency decades of data points were used, corresponding to the partial low frequency semicircle in the diagram. The results provide rough estimates of apparent corrosion rates, often only indicative of an upper bound of corrosion rate. Therefore, the results are reported as an ACR. For concrete resistivity measurements, only the high frequency part of the EIS diagrams was used, adopting for the value of Rs the real part of the impedance at the point of lowest imaginary component, before the onset of the region that eventually forms the low frequency loop, coinciding with the end of the high frequency loop if that one was readily apparent.

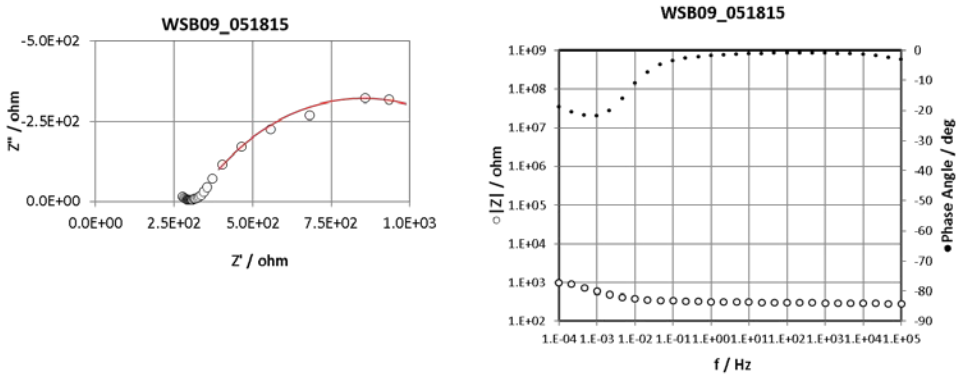


Figure 25: Output of EIS Data for Sandblasted Specimen Exposed to Salt Water at ~1 Month of Exposure. Line in the Nyquist Diagram Represents Computer Fit to Lowest 2 Decades of Frequency Data. Fit Rp Value was 1.3 k ohm. After Accounting for Specimen Surface Area ACR was 5.8 μm/y. Value of Rs for Estimating Concrete Resistivity was ~260 ohm.

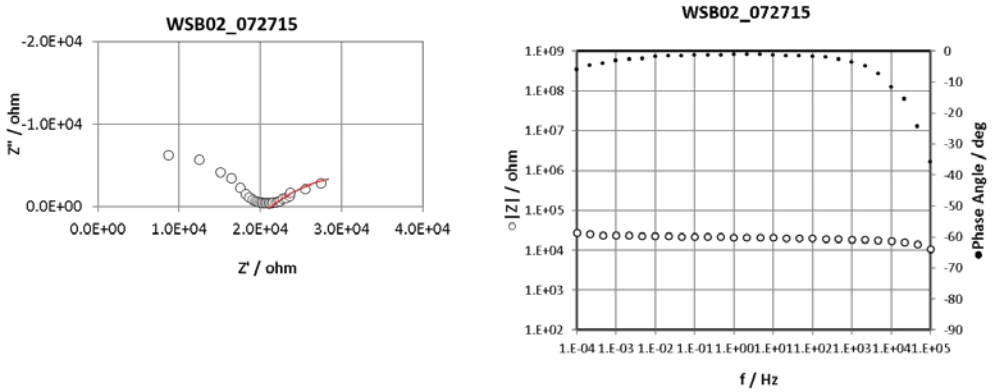


Figure 26: Output of EIS Data for Sandblasted Specimen Exposed to Fresh Water at ~3 Months of Exposure. Line in the Nyquist Diagram Represents Computer Fit to Lowest 2 Decades of Frequency Data. Fit Rp Value was 43 k ohm. After Accounting for Specimen Surface Area ACR was 0.18 μm/y. Value of Rs for Estimating Concrete Resistivity was ~20,000 ohm.

Figures 27 and 28 illustrate the ACR values as function of time of exposure determined for all specimens by the analysis indicated above. For 85% RH exposures only very limited data were available due to high uncertainty in evaluating EIS spectra in high resistivity media. Nevertheless the available results, indicated extremely low ACR values for the not epoxy-coated specimens in this environment (< 0.15 μm/y), consistent with the potential measurements indicative of passive behavior. For epoxy-coated specimens the ACR was even smaller than for the other conditions.

For fresh and mild water exposure, the not epoxy-coated specimens showed ACRs that near the end of the test period were greater than those for the 85% RH condition, but with values still only about 0.3 to 2 μm/y. For salt water exposure the ACR values for not epoxy-coated specimens were, surprisingly, not dramatically higher than those in the fresh and mild water regimes.Variations of ACRs with time appeared to indicate a modest decreasing trend in some of the cases, but longer term testing will be needed for confirmation. The EIS results for all the immersion regimes were consistent with the OCP measurements, which showed early activation of the specimens, albeit the ACRs in these cases turned out to be quite low. In all exposure categories ACR for Epoxy Coated bars were extremely small, as much as two orders of magnitude lower than those for the other conditions. It is noted, however, that for epoxy coated rebar the EIS method may not be able to sufficiently detect any corrosion that could be taking place at the metal-coating interface around the existing small coating breaks, so specimen autopsy will be necessary to examine that possibility.

Figure 29 shows a comparative summary of the ACR at approximately 5 months of exposure, consistent with the above observations. Notably, for all exposure regimes there was no clearly evident differentiation observed between the ACR behavior of the Mill Scale and Sandblasted specimens.

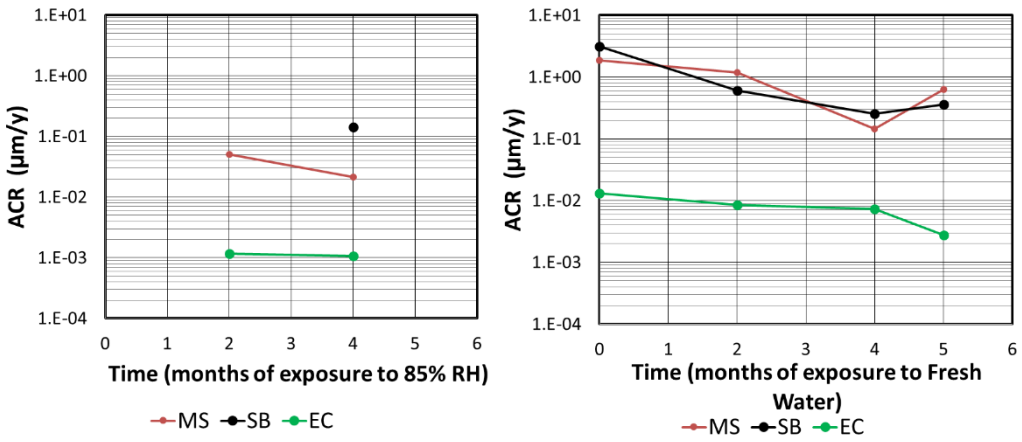


Figure 27: CR of Specimens Exposed to 85% RH and Fresh Water

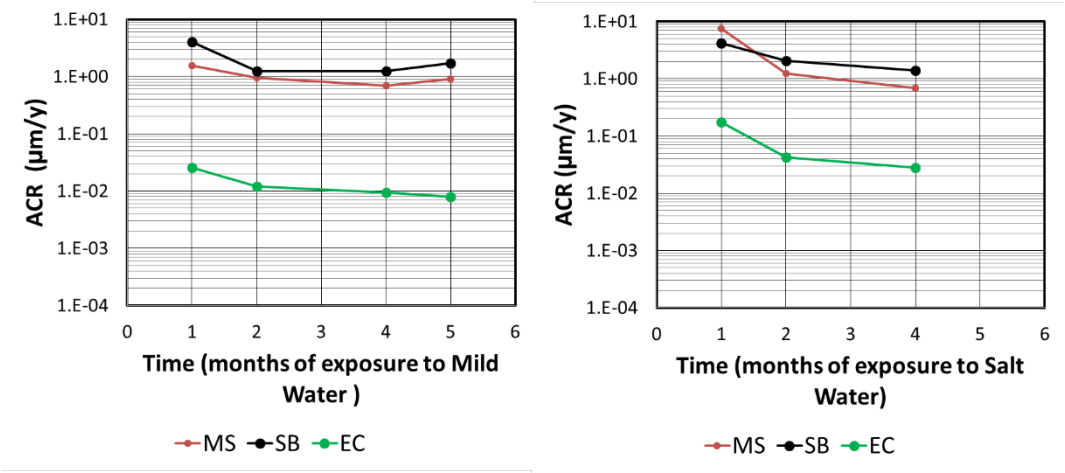


Figure 28: CR of the Specimens Exposed to Mild Water and Salt Water

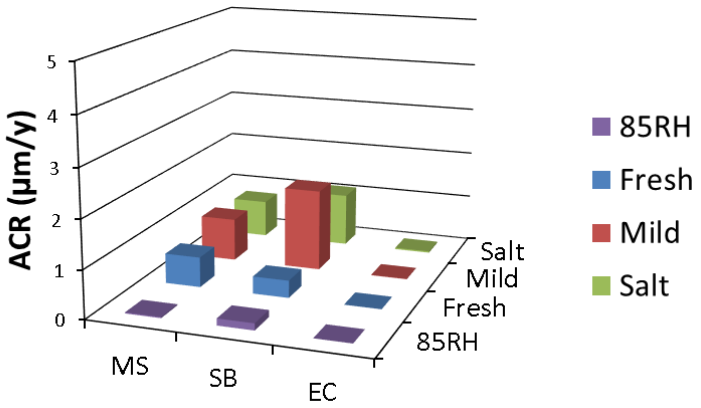


Figure 29: Summary of ACR after ~5 Months of Exposure

**Concrete Resistivity**

Figure 30 shows the values obtained for the concrete resistivity. As discussed in more detail later, compared with the values commonly encountered in chloride free OPC concrete [37], resistivity of this particular SC-concrete type was very high for the immersed portion of the specimens in fresh and mild water environments ( ~1 order of magnitude higher), and extremely high for the specimens in the 85% RH chamber (over 2orders of magnitude higher). Only the immersed portion in the salt water solution developed relatively low resistivity values, comparable to those of a medium permeability OP concrete [37].

Note that as expected, the results were about the same for all types of bare metal rebar finish, since the resistivity is a property of the concrete and not of the embedded rebar which, for this parameter test, served only as a current and potential measuring electrode. Interfacial polarization of the steel is not important at the typical frequency giving Rs in the EIS diagram. No values are reported for EC rebar specimens as the insulating epoxy coating introduces added resistance not included in Equation 11.

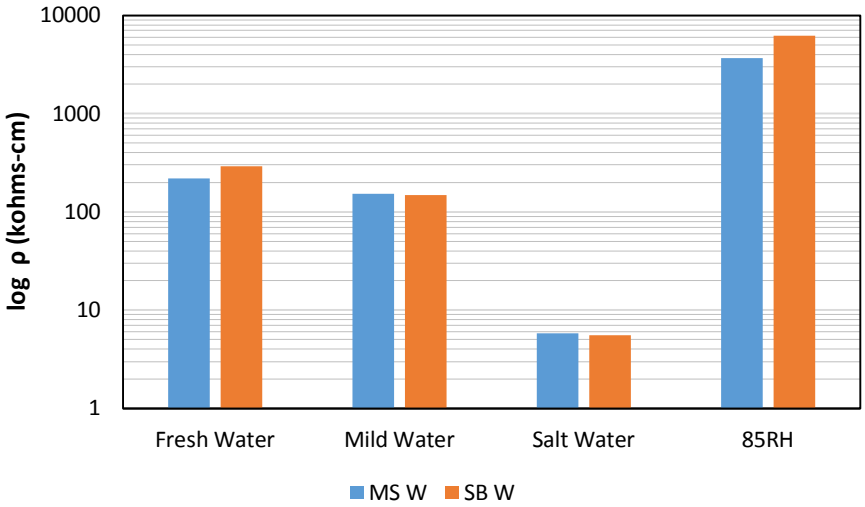


Figure 30: Concrete Resistivity Measured Using the Indicated Rebars as Electrodes

The Resistivity Formation Factor [38] of a porous solid or resistivity Rp filled with a fluid or resistivity Rf is defined as:

$$RFF = \frac{Rp}{Rf} \tag{13}$$

For many tightly porous solids with medium-low porosity and a relatively inert, low solubility matrix (for example natural limestone), RFF is on the order of several hundred. RFF was calculated for the present specimens, assuming that during the exposure period to date, the external solution has permeated through most of the pore network of the submerged part, results are shown in Table 3.

Table 3: RFF (Average of Results for each Immersed Regime)

| Water Solution | Solution Conductivity mS/cm | Solution Resistivity kohm-cm | Concrete Resisitivity kohm-cm | Approximate Resistivity Formation Factor |
|---|---|---|---|---|
| **Fresh** | 0.2 | 5.00 | 236 | 47 |
| **Mild** | 0.55 | 1.82 | 150 | 83 |
| **Salt** | 63 | 0.02 | 6 | 378 |

The SC-concrete type examined here displayed RFF values that are on the order of those expected for relatively inert natural materials with appreciably low porosity and tortuosity [39]. These findings support the internal consistence of the results to date and expectations of sustaining very high concrete resistivity in exposure environments with water of low to moderate ionic content.

**Relative Porosity**

Figure 31 shows the water uptake for one of the specimens evaluated. As can be seen, the water uptake reached ~50% of saturation level after approximately only 3 days, suggesting very fast water pickup. The estimated volumetric porosity not filled with water in the as-received condition was 5.0 %, with a standard deviation of 0.2%. The separate experiments in which as-received specimens were oven-dried indicated that the as-received evaporable water content was ~1 % of the specimen mass, corresponding to about 2.6 % of the specimen volume. Hence the overall volumetric porosity estimated by these specimens is 7.6%.

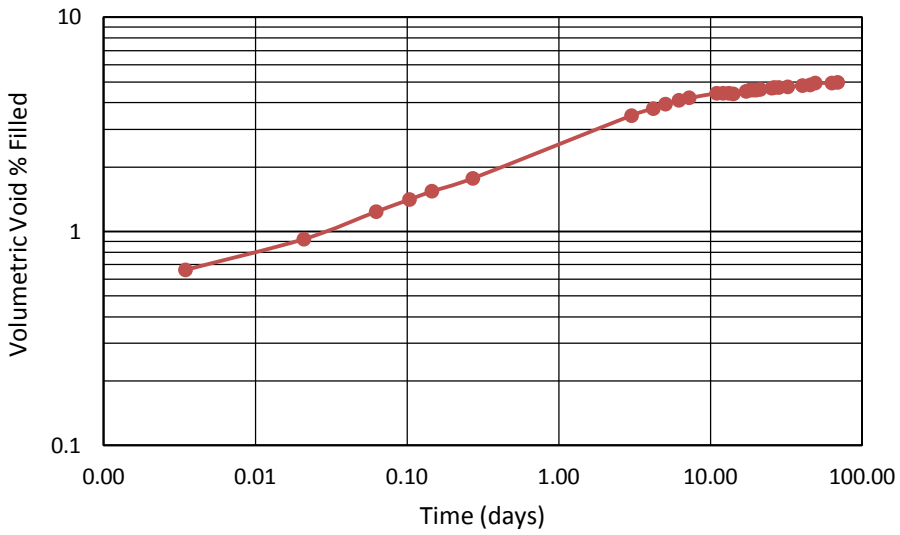


Figure 31: Example of Void Volume (As Percentage of Specimen Volume) Filled as Function of Time by Absorbed Water in an Immersion Test Conducted with an As-Received Specimen of the Developmental Variation of SC-Concrete Investigated. Absorption Reached a Plateau at ~ 5%. Initial Moisture-Filled Porosity was ~2.6% Based on Tests in Other Specimens.

**Weight Gain in Test Media**

Figure 32 shows the results obtained for the weight gain during exposure to the test media for selected specimens. For the immersion regimes, it can be seen that after three days the specimens gained 1% weight, approaching 2.5% after 1000 hours. From the standpoint of possible reinforcement susceptibility to corrosion such water pickup rate may be considered to be very fast, and is consistent with the early onset of activation seen in the immersion regimes. The specimens that gained ~3.5% weight were exposed to salt water, with salt efflorescence (not bulk absorption) accounting for the excess weight presented. For the specimens exposed to 85% RH the water uptake was only ~1% after 100 days, by which time the weight had reached a steady - state regime. As it will be shown below, the native internal humidity of the SC-concrete type assessed here is not much different from 85%, hence the small weight change in this medium.

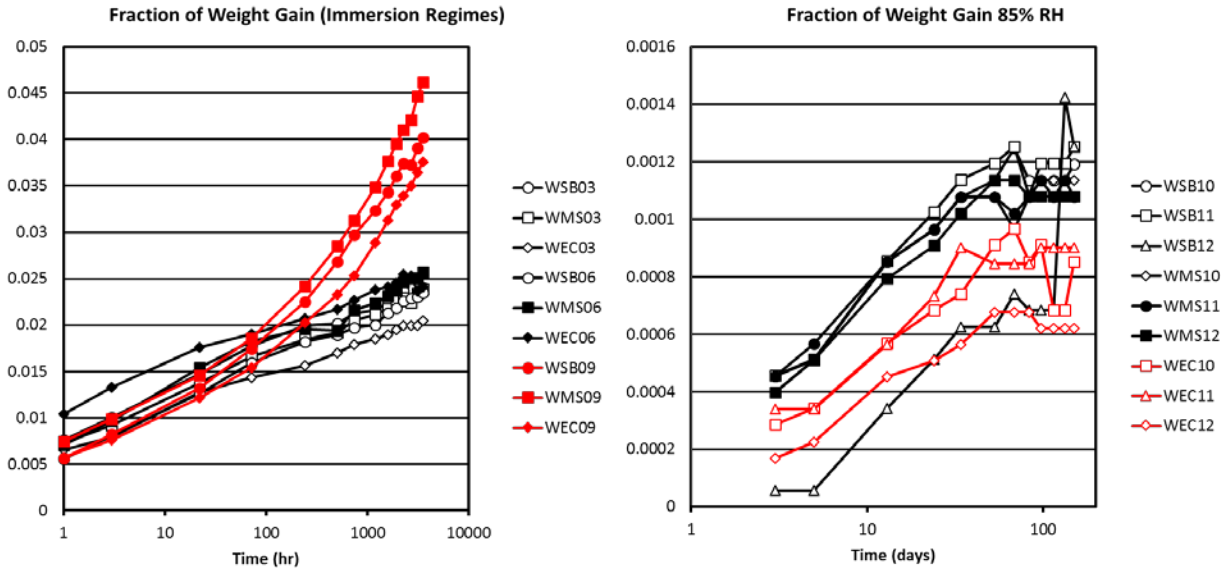


Figure 32: Fraction of Weight Gain for Exposure Regimes

**Native Internal Humidity**

Figure 33 shows a summary of the native internal humidity results. The duplicate specimens were exposed to the specified relative humidity environments for ~85 days. All the data from each environment were gathered and analyzed to graphically determine the point where there was not net gain or loss (K=0). That points indicates the moisture content of the material.

Note that the reinforced concrete specimens exposed to a relative humidity of 85% (used only data for the first 24 days) had a small positive K value and the plain concrete specimens exposed to the same environment had a small negative K value. In absolute terms this difference was very small and could possibly be attributed to the fact that the blank and the reinforced specimens came from different SC-concrete production batches.

In general, specimens exposed to a relative humidity equal or lower than 85% had a negative K value and the specimens exposed to a relative humidity equal or higher than 85% had a positive K value. For this developmental variation of SC-concrete, the native moisture content was therefore estimated to be ~85%.

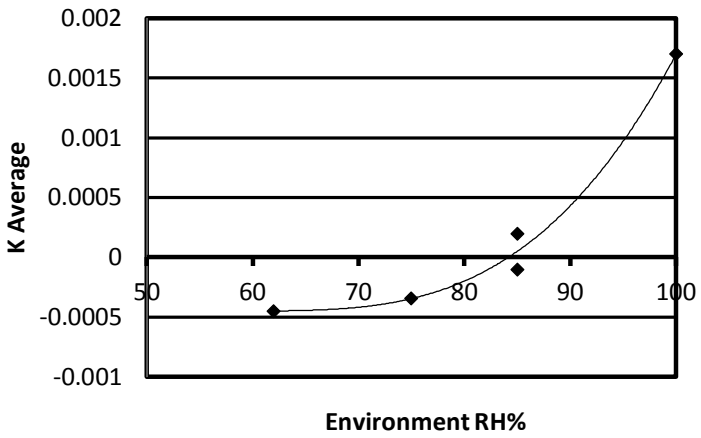

Figure 33: Native Humidity Results Summary

**pH of the Pore Water**

Figure 34 illustrate a schematic for the arrangement of the holes in the concrete and Figure 35 shows one example of the results obtained. After ~ 10 days of exposure of the two selected specimens for pore water pH determination a first set of measurements was taken by using an activated titanium microelectrode and a silver-silver chloride (SSC) reference electrode at laboratory temperature (~25 +/- 3 °C).

The ISL method was performed until no significant variation of pH was encountered. The pH obtained from an average of 4 values at 2.5 weeks of exposure was 8.8 with a standard deviation of 0.2. It was noted that stabilization occurred towards higher pH values.

## CHAPTER 5: SIGNIFICANCE OF FINDINGS

### Corrosion Rate Considerations

The array of experimental methods deployed in this investigation provided useful insight on the corrosion behavior of reinforcement in this novel material.

The behavior of not-epoxy coated reinforcement will be considered first. As the experiments did not show strong differentiation between the mill scale and sandblasted conditions the following comments will be considered to apply to both categories equally. The ACR values obtained are compared in Figure 36 to typical corrosion rates illustrated by Gonzalez et al. [22] for a number of exposure conditions for reinforcement embedded in OCP concrete when the reinforcement is in the passive condition, and for various conditions after the active corrosion propagation stage has started.

Specimens exposed to 85% R.H., a condition which is of interest for service that may involve sheltered structural components with exposure to moisture but no direct water contact, showed indications of extended preservation of the passive condition and extremely low ACRs; those values fall well within the range indicated by Gonzalez et al. for the passive condition in OPC.

Exposure to the Fresh Water regime resulted in rapid indications of steel activation, but despite that the ACRs, while finite, were quite small and after a few months of exposure the values obtained were not much above those typical of passive steel in OPC, or at the very low end of the range of corrosion rates encountered for actively corroding steel in OPC.

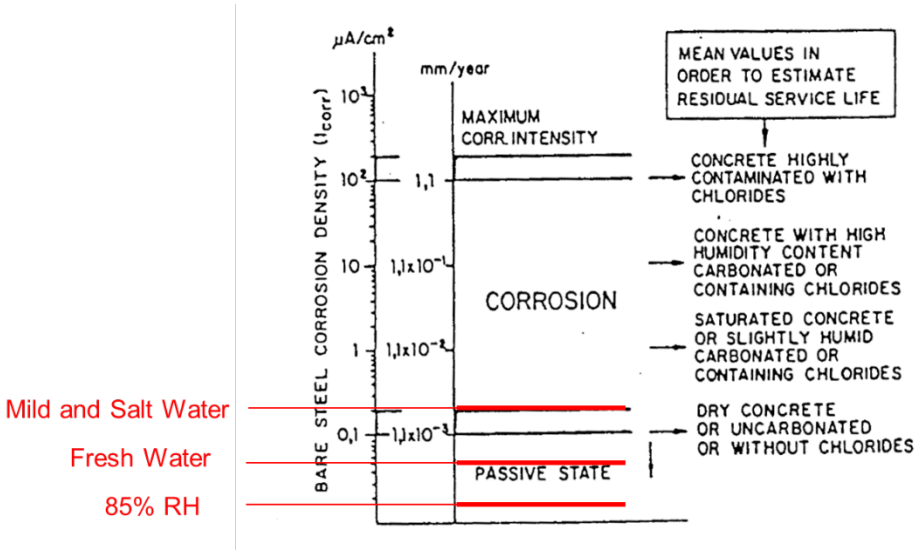


Figure 34: ACR Comparison between SC-Concrete and OPC-Concrete. Source: Gonzalez. et al. [22]

Exposure to the mildly aggressive water regime also resulted in evidence of rapid early activation, but the subsequent ACR values tended to be very modest, comparable to those seen at the low end of corrosion rates for carbonated OCP without chloride contamination and low moisture content. The ACR values for this regime were lower than those typical of humid carbonated concrete, which would have been considered otherwise to be a corrosion analog for SC-concrete as noted earlier [22].

Surprisingly, exposure in the salt water regime, which also resulted in clear signs of early steel activation, yielded ACR values that while moderately high at the beginning, tended to stabilize later on toward small values comparable to those of the mild water regime. Those values are much lower than the corrosion rates often observed for partially aerated, highly humid, highly chloride contaminated OPC during the corrosion propagation stage, as cited by Gonzalez. A possible explanation for this behavior is discussed later.

The ACR of epoxy coated steel was extremely low in all cases. However, as noted earlier in this case specimen autopsies are essential to ascertain that the indications of low ACRs are not a result of limitation of the EIS tests to detect undercoating corrosion [40]. Therefore, further

discussion of this material as a possible corrosion control approach for SC-concrete will be left for future consideration after additional evidence is obtained.

The results for the regular rebar will also require confirmation by autopsy examination of selected specimens after a longer test time has been accrued. Nevertheless, possible artifacts complicating interpretation of EIS assessment are less likely than in the case of epoxy coated rebar and some initial impressions may be indicated as follows.

***Prospects for Corrosion Performance of Plain Rebar***

The following comments are based on the short period of evaluation to date and therefore must be viewed only as preliminary impressions, subject to later evaluation over longer test periods followed by autopsy of the specimens. Nevertheless, some valuable insights may be made at this stage and are presented here with the understanding that the above caution applies.

For atmospheric exposure in moderately moist environments (e.g. the 85% RH test condition) the corrosion performance of plain steel in the SC-concrete type examined appears to be promising. This result is encouraging for applications, such as indoor hollow slabs and similar structural components, not subject to direct wetting.

Direct exposure to the fresh and the slightly aggressive mild water media did result in nearly immediate initiation of active corrosion, indicative of a very short corrosion initiation stage. This interpretation is consistent with the observation of a very fast water penetration mechanism, as observed in the specimens that were monitored for weight gain under partial immersion. The mildly alkaline character of the pore water plays a role in this early activation as well: with the increase in moisture, and without a passive film to avoid the anodic reaction, all the key components that must be present for corrosion to occur are present and therefore the system experiences corrosion propagation already at the early stages of service.

The corrosion behavior in these environments therefore appears to be dictated predominantly by performance during the propagation stage. The ACRs were very low, however, on the order of only < 2 μm/y. Those values are nevertheless not negligible, as such rates might result in corrosion induced cracking after as little as a decade or as much as some decades of service, much as for OPC concrete after the end of the corrosion initiation period [9] in situations of moderate to low corrosion rates. If the behavior shown in the short tests reported in this thesis is confirmed by extended testing, applications for contact with fresh natural water where service life is needed for only moderate periods might be achievable without any additional corrosion protection provisions.

Overall, the behavior observed suggests that, despite the rapid activation of the steel surface, other properties of the developmental variation of the SC-concrete evaluated, such as its very high resistivity, may be acting as factors strongly mitigating the corrosion process. In that context, the concrete type assessed here exhibited very high resistivity in the Fresh Water and Mild Water tests, and extremely high resistivity in the 85% RH moist atmospheric exposure compared to a selection of typical values for water-saturated OPC (Figure 37) [41]. Such high resistivity can introduce large amounts of electric resistance polarization, especially of the anodic reaction, when corrosion macrocells are the main modality of corrosion distribution on the steel surface thus accounting at least in part for the very low ACR values observed.

Caution applies however on some issues that could lead to overoptimistic interpretation of the observed ACR values. In particular, the high resistivity of the medium may result in EIS underestimation of the corrosion rate of small localized active regions [42]. Additionally, given the tendency of the concrete assessed for rapid and strong water absorption observed earlier, the partial immersion regime might have resulted in a greater degree of water saturation in the upper

parts of the test specimens than initially anticipated. The extent of diffusional polarization of the cathodic oxygen reduction reaction could have accordingly been greater with consequent decrease of the overall corrosion rate. The uncertainty from these possible causes requires resolution via terminal specimen autopsy as indicated earlier, and by follow up experiments such as temporary removal of specimens from the test tank to allow for water evaporation and concurrent EIS measurements to detect any significant changes.

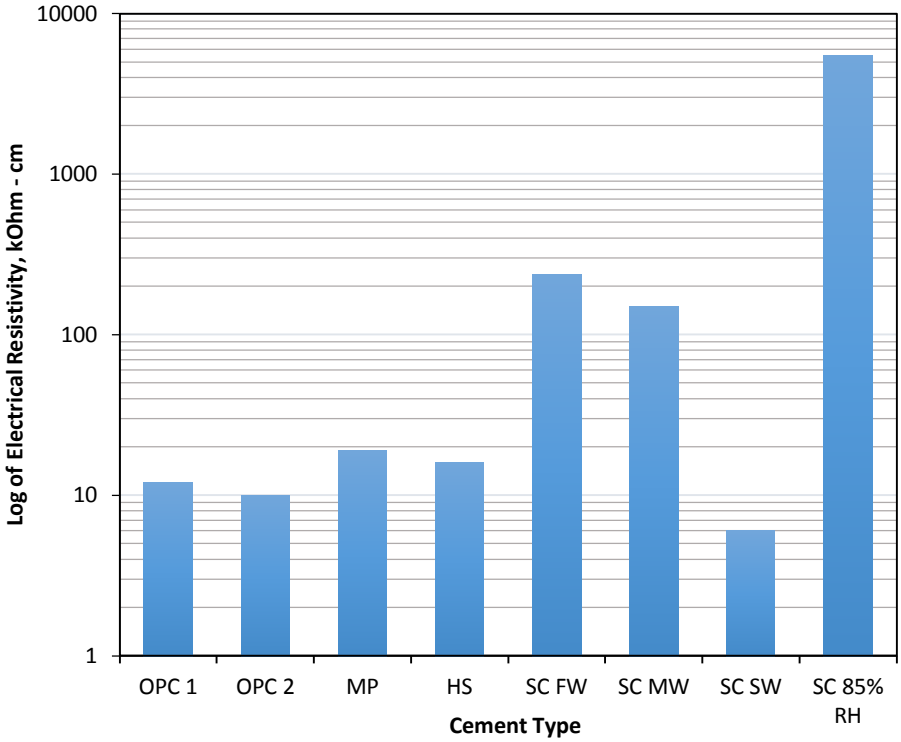


Figure 35: Influence of Cement Type on Electrical Resistivity of Saturated Concrete. In the Figure: OPC1, OPC2: Ordinary Portland Cement Saturated, MP: Modified Portland Cement Saturated (20% fly ash), HS: High Strength Portland Cement Saturated, SC FW: SC-concrete* saturated with fresh water, SC MW: SC-concrete* Saturated with Mild Water, SC SW: SC-concrete* Saturated with Salt Water, SC 85% RH: SC-concrete* exposed to 85% RH. (*of the type assessed in this investigation).

Direct exposure to the salt water medium resulted in nearly immediate activation as well with the same implications noted above for the fresh/mild water group. The ACRs were initially notably greater that those of the previously discussed group, as expected given the highly aggressive nature of the medium. Those ACR values, if sustained, would cause concrete cracking in an OPC application in a short time, on the order of only a few years. The ACRs decreased rapidly however, to values comparable to those of the mild water group. This decrease in such otherwise aggressive environment must be carefully examined for possible artifacts in the light of the concerns discussed earlier. Underestimation of corrosion rates from EIS resistivity artifacts is less likely than in the fresh/mild water experiments as in salt water the SC type assessed here exhibited, as expected, resistivity values that were not very large (Figure 37). The other artifact mentioned, excessive water pickup, merits more attention as the evaporative salt accumulation might have assisted more water pickup via deliquescence. As indicated above, longer term resolution of uncertainty will require terminal autopsy and temporary drying/EIS assessments.

**Methodology Considerations**

It is emphasized that the experiments addressed in this Thesis are only one component of a more extended group of evaluations of developmental variations of SC-concrete and other alternative rebar conditions. Nevertheless, the evaluations served to illustrate the array of methodologies that can be deployed to evaluate the corrosion performance of reinforcement in new media and provide a framework for extended investigations. As indicated before, prolonged evaluation and terminal autopsies beyond these initial months of exposure will be required for a more definitive assessment of corrosion related durability.

**Follow Up Work**

As indicated in the above discussion, extension of this work to achieve longer exposure times (e.g. one year or more).is needed to ascertain the early behavior trends identified so far.

Autopsy of the specimens is anticipated to validate electrochemical impedance data. Specifically in the case of EC rebar where is necessary to determine if corrosion was taking place underneath the coating.

Additional experiments where specimens exposed to immersion in salt water are allowed to dry for a period of time to evaluate possible impact in corrosion rates are also anticipated.

Work should be also extended to other developmental formulations of the SC-concrete and surface conditions to expand the assessment matrix and provide valuable information related with the potential durability of the reinforced concrete.

## CHAPTER 6: CONCLUSIONS

Reinforced concrete made with a developmental type of Solidia Cement™ (SC) concrete and plain steel rebar in the as received and sandblasted condition, as well as epoxy coated rebar was evaluated for about 5 months for corrosion behavior in air at 85% RH and partial immersion regimes with fresh water, mild water and salt water. The main findings of this study are indicated below:

- Specimens exposed to air at 85% RH appeared to retain a passive steel condition during the entire exposure period. Apparent corrosion rates (ACR) derived from electrochemical impedance spectroscopy (EIS) were extremely low. Pending confirmation by prolonged testing, this result is encouraging for applications such as indoor hollow slabs and similar structural components not subject to direct wetting.
- Specimens exposed to immersion regimes in Fresh, Mild and Salt water media showed signs of activation after a very short time (days-week) of exposure. Corrosion assessment thus occurred predominantly in the corrosion propagation stage. Early activation is thought to reflect a combination of rapid water absorption and only moderately alkaline pH (~8.8) of the concrete assessed.
- The ACRs for plain and sandblasted rebar in the Fresh and Mild water regimes were very low, e.g, < 2 μm/y. If confirmed by further evaluation, applications for contact with fresh natural water where service life is needed for only moderate periods might be achievable. The SC-concrete assessed here exhibited much higher resistivity values than conventional

PC concrete in similar conditions. This higher resistivity may have been an important factor in limiting corrosion rate.

- ACRs of plain and sandblasted rebar in the salt water exposure were initially notably greater that those indicated above, as expected given the highly aggressive nature of the medium. Those ACR values, if sustained, would cause concrete cracking in an OPC application in a short time, on the order of only a few years. ACRs however decreased with exposure time but those results need careful follow up evaluation for possible artifacts such as excessive water pickup from salt deliquescence, which could have transport-limited the rate of the cathodic reaction.
- ACRs of epoxy-coated rebar specimens (which had 0.25% intentional surface flaws) were extremely small in all test conditions. However, this result may stem from limitations of the EIS tests to detect undercoating corrosion and interpretation of this finding needs to be postponed until future autopsy of test specimens.

## REFERENCES


1. Online, E.B., *Cement*. 2015, Encyclopedia Britannica Inc.

2. Scrivener, K., *Options for the future of cement.* Indian Concrete Journal, 2014. **88**(7): p. 11-21.

3. Mindess, S., J.F. Young, and D. Darwin, *Concrete*. 2003: Prentice-Hall Inc. New Jersey.

4. Oxygen, P. *CO2 Now*. 2015 12 February 2015]; Available from: http://co2now.org/Current-CO2/CO2-Now/global-carbon-emissions.html.

5. Gibbs, M.J., P. Soyka, and D. Conneely, *CO2 Emissions from Cement Production*, in *Good Practice Guidance and Uncertainty Management in National Greenhouse Gas Inventories*. 2000, IPCC.

6. Solidia Technologies. *Sustainability and Profitability*. 2015 [cited 2015; Available from: http://solidiatech.com.

7. Solidia Technologies. *Water Savings in Concrete made from Solidia Cement*. 2014 [cited 2015; White Paper. Available from: http://solidiatech.com.

8. Fontana, M.G., *Corrosion engineering*. 2005: McGraw-Hill Education

9. Bentur, A., N. Berke, and S. Diamond, *Steel corrosion in concrete: fundamentals and civil engineering practice*. 1997: CRC Press.

10. Andrade, M. and S. Feliu, *Corrosión y protección metálicas* Vol. 1. 1991, Madrid: Consejo Superior de Investigaciones Científicas.

11. Sagüés, A.A. *Corrosion measurement techniques for steel in concrete.* Paper No. 353, Corrosion/93, NACE International, Houston.

12. Tuutti, K., *Corrosion of steel in concrete*. 1982: Swedish Foundation for Concrete Research. 469.

13. Cabrera, J., *Deterioration of concrete due to reinforcement steel corrosion.* Cement and concrete composites, 1996. **18**(1): p. 47-59.

14. Diamond, S., *Aspects of concrete porosity revisited.* Cement and Concrete Research, 1999. **29**(8): p. 1181-1188.

15. Swamy, R.N. *Corrosion and Corrosion Protection of Steel in Concrete: proceedings of International Conference held at the University of Sheffield, 24-28 July 1994; volumes I and II*. in *Corrosion and Corrosion Protection of Steel in Concrete, International Conference, 1994, University of Sheffield, United Kingdom*. 1994.

16. Sandberg, P., *Durability of concrete in saline environment*. 1996: Cementa AB. 206.

17. Deltombe, E., N. De Zoubov, and M. Pourbaix, *Atlas of electrochemical equilibria in aqueous solutions.* Pergamon Press, 1974. **Section 5**: p. 168.

18. Sagüés, A.A., *Electrochemical Impedance for Measuring Corrosion of Steel in Reinforced Concrete (in spanish)*, in *Corrosion Metalica Proceedings, 1st International Workshop on Corrosion*. 1992, L. Maldonado, P. Castro and L. Diaz, Eds.: CINVESTAV Merida.

19. Jones, D., *Principles and prevention of corrosion.* Prentice-Hall Inc., Upper Saddle River, NJ, 1996: p. 76-90.

20. GAMRY. *Echem Analyst Software*. [cited 2015 10/08]; Available from: http://www.gamry.com/assets/Support-Downloads/Quick-Start-Guides/EchemAnalystSoftwareManual.pdf.

21. Sagüés, A., E. Moreno, and C. Andrade, *Evolution of pH during in-situ leaching in small concrete cavities.* Cement and Concrete Research, 1997. **27**(11): p. 1747-1759.

22. Andrade, C. and C. Alonso, *Values of Corrosion Rates of Steel in Concrete to Predict Service Life of Concrete Structures*. ASTM STP 1194, American Society for Testing and Materials. 1994, Philadelphia: Gustavo Gragnolino and Narasi Sridhar, Eds.

23. Sagüés, A.A., et al., *Carbonation in concrete and effect on steel corrosion*. Final report to Florida Department of Transportation, Report No. 99700-3530-119. 1997, FDOT: Tallahassee, FL.

24. EPA, *Hydrogen Sulfide Corrosion in Wastewater Collection and Treatment Systems*. 1991: Washington, DC.

25. Ray, R.I., J.S. Lee, and B.J. Little, *Iron-oxidizing bacteria: a review of corrosion mechanisms in fresh water and marine environments*. 2010, DTIC Document.

26. Wei, S., et al., *Microbiologically induced deterioration of concrete: a review.* Brazilian Journal of Microbiology, 2013. **44**(4): p. 1001-1007.

27. ASTM. *Standard Specification for Deformed and Plain Carbon-Steel Bars for Concrete Reinforcement A615*. ASTM.

28. ASTM. *Standard Specification for Epoxy-Coated Steel Reinforcing Bars A775*. ASTM.

29. FDOT, *Standard Specifications for Road and Bridge Construction*. 2012: Florida Department of Transportation.

30. Barnes, H., *Some tables for the ionic composition of sea water*. Journal of experimental biology, 1954. **31**(4): p. 582-588.

31. Castro, P., et al., *Characterization of activated titanium solid reference electrodes for corrosion testing of steel in concrete.* Corrosion, 1996. **52**(8): p. 609-617.

32. McPherson, L., *Using correct conductivity temperature compensation.* Water/Engineering and Management, 1997. **144**(5): p. 36-44.

33. Pech-Canul, M., A. Sagues, and P. Castro, *Influence of counter electrode positioning on solution resistance in impedance measurements of reinforced concrete.* Corrosion, 1998. **54**(8): p. 663-667.

34. Young, J.F., *Humidity control in the laboratory using salt solutions—a review.* Journal of Applied Chemistry, 1967. **17**(9): p. 241-245.

35. ASTM. *Standard Test Method for Density, Absorption, and Voids in Hardened Concrete C642*. 2001. ASTM Philadelphia, PA.

36. Moreno, E.I. and A. Sagüés. *Carbonation-induced corrosion of blended-cement concrete mix designs for highway structures*. Paper No. 636, Corrosion/98, NACE International, Houston.

37. Sagüés, A.A., et al., *Corrosion Forecasting for 75-Year Durability Design of Reinforced Concrete*. Final report to Florida Department of Transportation, Report No. BA502. 2001, FDOT: Tallahassee, FL.

38. Crain, E.R. *Crain's petrophysical handbook*. 2000; Available from: http://www.spec2000.net.

39. Wong, P.-z., J. Koplik, and J. Tomanic, *Conductivity and permeability of rocks.* Physical Review B, 1984. **30**(11): p. 6606.

40. Sagüés, A.A., et al., *Corrosion of Epoxy-Coated Rebar in Marine Bridges-Part 1: A 30-Year Perspective.* Corrosion, 2010. **66**(6): p. 065001-065001-13.

41. Elkey, W. and E.J. Sellevold, *Electrical resistivity of concrete.* Norwegian Public Roads Administration, 1995. **80**: p. 33.

42. Sagüés, A.A. and S. Kranc, *Computer Modeling of Effect of Corrosion Macrocells on Measurement of Corrosion Rate of Reinforcing Steel in Concrete*. In Techniques to Assess the Corrosion Activity of Steel Reinforced Structures, ASTM STP 1276. American Society for Testing and Materials. 1996: Neal S. Berke, Edward Escalante, Charles Nmai and Favid Whiting, Eds.

## APPENDIX A: LIST OF SYMBOLS

| | |
|---|---|
| ACR | Apparent Corrosion Rate |
| Cdl | Interfacial Capacitance of the Steel |
| CSE | Saturated Calomel Electrode |
| EC | Epoxy Coated |
| EIS | Electrochemical Impedance Spectroscopy |
| FW | Fresh Water |
| MIC | Microbial Induced Corrosion |
| MW | Mild Water |
| MS | Mill Scale |
| OPC | Ordinary Portland Cement |
| PC | Portland Cement |
| RFF | Resistivity Formation Factor |
| RH | Relative Humidity |
| Rp | Polarization Resistance |
| Rs | Electrolyte Resistance |
| SC | Solidia Cement |
| SW | Salt Water |
| SB | Sandblasted |

## APPENDIX B: COPYRIGHT PERMISSIONS

Below is permission for the use of Figure 34.

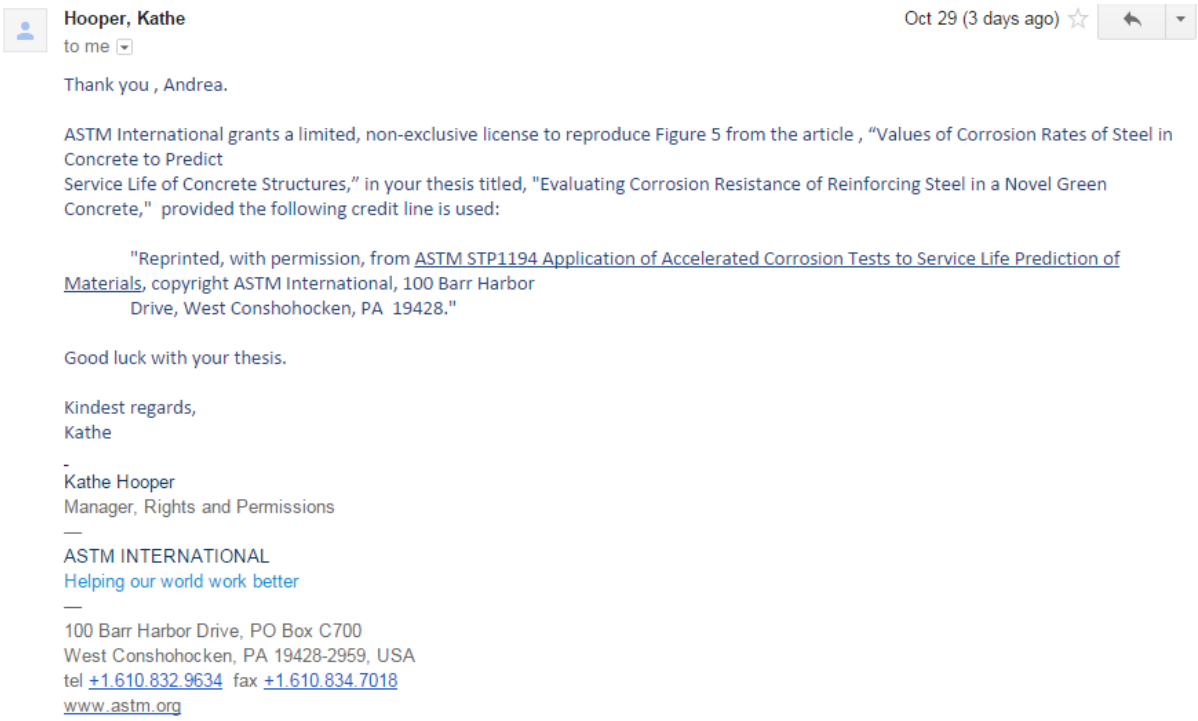

**Hooper, Kathe** Oct 29 (3 days ago)
to me

Thank you , Andrea.

ASTM International grants a limited, non-exclusive license to reproduce Figure 5 from the article , "Values of Corrosion Rates of Steel in Concrete to Predict
Service Life of Concrete Structures," in your thesis titled, "Evaluating Corrosion Resistance of Reinforcing Steel in a Novel Green Concrete," provided the following credit line is used:

"Reprinted, with permission, from ASTM STP1194 Application of Accelerated Corrosion Tests to Service Life Prediction of Materials, copyright ASTM International, 100 Barr Harbor Drive, West Conshohocken, PA 19428."

Good luck with your thesis.

Kindest regards,
Kathe

-
Kathe Hooper
Manager, Rights and Permissions
—
ASTM INTERNATIONAL
Helping our world work better
—
100 Barr Harbor Drive, PO Box C700
West Conshohocken, PA 19428-2959, USA
tel +1.610.832.9634 fax +1.610.834.7018
www.astm.org